

# Three-outcome multipartite Bell inequalities: applications to dimension witnessing and spin-nematic squeezing in many-body systems

Guillem Müller-Rigat,<sup>1,\*</sup> Albert Aloy,<sup>2,3</sup> Maciej Lewenstein,<sup>1,4</sup> Matteo Fadel,<sup>5,†</sup> and Jordi Tura<sup>6,7,‡</sup>

<sup>1</sup>*ICFO-Institut de Ciències Fotoniques, The Barcelona Institute of Science and Technology, Castelldefels (Barcelona) 08860, Spain.*

<sup>2</sup>*Institute for Quantum Optics and Quantum Information, Austrian Academy of Sciences, Boltzmannngasse 3, A-1090 Vienna, Austria*

<sup>3</sup>*Vienna Center for Quantum Science and Technology (VCQ), Faculty of Physics, University of Vienna, Vienna, Austria*

<sup>4</sup>*ICREA, Pg. Lluís Companys 23, 08010 Barcelona, Spain.*

<sup>5</sup>*Department of Physics, ETH Zürich, 8093 Zürich, Switzerland*

<sup>6</sup>*(aQa<sup>L</sup>) Applied Quantum Algorithms, Universiteit Leiden*

<sup>7</sup>*Instituut-Lorentz, Universiteit Leiden, P.O. Box 9506, 2300 RA Leiden, The Netherlands*

We present a three-outcome permutationally-invariant Bell inequality, which we show to be naturally suited to explore nonlocal correlations in many-body spin-1 systems or SU(3) models. In the specific, we show how to derive from this inequality experimentally practical Bell correlation witnesses based on the measurement of collective spin components. Moreover, we present approaches that allow us to derive scalable Bell dimension witnesses, namely criteria whose violation signals the impossibility of reproducing the observed statistics by single-particle Hilbert spaces of a certain dimension. This enables the certification of genuine three-level correlations that cannot occur in two-level, i.e. qubit, systems. As an example, we show the application of these witnesses in spin-nematic squeezed states, such as the one that can be prepared in spin-1 Bose-Einstein condensates.

## I. INTRODUCTION

The formalism of quantum mechanics brought revolutionary ideas that challenged preconceived notions in classical physics, such as causality, locality and realism. A characteristic feature of quantum mechanics is that any complex linear combination of two valid quantum states results in another valid, qualitatively different, quantum state. Moreover, when considering many-body quantum systems, such characteristic feature may lead to correlations that violate the principles of locality and realism [1], resulting in one of the strongest departure from classical physics. In 1964, the seminal work of J. S. Bell offered a precise mean to characterize correlations that follow local-realistic principles by formalizing local hidden variable models and, in turn, the so-called Bell inequalities [2]. Correlations that violate a Bell inequality are incompatible with local hidden variable theories, and are thus called nonlocal.

Nowadays, nonlocal correlations constitute one of the building blocks of modern physics [3]. Besides their role in the history of quantum mechanics [1, 2] and their fundamental interest [4–6], these correlations have driven a paradigm shift in quantum protocols [7] by introducing Device-Independent (DI) Quantum Information Processing tasks [8]. That is, tasks that do not require trust nor knowledge about their physical implementation. For instance, nonlocality serves as a resource for DI tasks such

as self-testing [9–12], randomness amplification and expansion [13, 14], DI quantum key distribution [8, 15] or DI detection and certification of entanglement [16–20] or nonlocality depth [21].

From a more applied perspective, recent progresses in quantum technologies, such as in quantum computing and simulation, have reached control over large-scale quantum systems composed by hundreds of constituent elements [22]. What makes these platforms depart from their classical analogue are genuine quantum resources, e.g. entanglement and nonlocality. It is thus extremely relevant the scalable detection and characterization of quantum correlations in these controllable many-body systems [23].

However, revealing nonlocal correlations is notoriously hard, especially in multipartite scenarios. The underlying mathematical complexity [24] (NP-complete in the general case [25]) has impeded a full characterization of nonlocality beyond the simplest scenarios [26–28]. Nevertheless, specific Bell inequalities have been designed for important classes of quantum states (*e.g.*, graph states [29–32], symmetric states [33, 34], continuous variable systems [35, 36], etc.), or Bell Inequalities with desirable properties have been put forward (*e.g.*, achieving maximal violation by maximally entangled [9, 10, 12] or partially entangled states [37–39]).

In order to be of interest for DI tasks, Bell inequalities need not only to be violated (*i.e.* detect nonlocality), but it is also desirable to have the possibility of characterizing which states and measurements yield their maximal quantum violation. This last feature is specially important in cryptographic or adversarial scenarios [40], as well as for DI protocols to yield optimal performance. Therefore, it is of the utmost importance to have Bell

\*Electronic address: [guillem.muller@icfo.eu](mailto:guillem.muller@icfo.eu)

†Electronic address: [fadelm@phys.ethz.ch](mailto:fadelm@phys.ethz.ch)

‡Electronic address: [tura@lorentz.leidenuniv.nl](mailto:tura@lorentz.leidenuniv.nl)

inequalities that can be implemented in many-body systems together with efficient optimization tools that allow to characterize their maximal quantum violation and how to achieve it.

In a series of works [41, 42], a successful approach to derive practical multipartite Bell inequalities (BI) was based on restricting to permutationally invariant (PI) few-body correlators. This allowed for the experimental detection of Bell correlations in many-body quantum systems using collective measurements only [43, 44]. Furthermore, such type of PIBI have allowed to explore the role of nonlocal correlations near critical points [45], or for quantum metrology [46]. On the other hand, the relatively simple structure of these PIBIs limits the type of states and physical systems in which nonlocality can be detected. Therefore, in order to overcome this limitation, it is interesting to derive PIBI of increased complexity, while still being of practical implementation [47–50]. For instance, this can be done by deriving PIBIs that involve more measurement settings [51], higher-order correlators [52], or more than two outcomes as we are going to do in this work.

Already for systems involving only two parties, the first derivation of a Bell inequality involving more than two outcomes [53] had fundamental implications in showing that entanglement and nonlocality are not equivalent, since maximally entangled states did not maximally violate the mentioned inequality. However, the derivation of multipartite Bell inequalities involving more than two outcomes remains largely unexplored, especially because of the underlying complexity of the problem. The increased number of outcomes results in a prohibitive scaling of the number of valid Bell inequalities, which makes their enumeration intractable. Therefore, even if some three-outcome multipartite Bell inequalities have been obtained [54], the state-of-the-art is far from being in a true many-body regime of experimental relevance.

Here, we derive and characterize a three-outcome Bell inequality tailored to many-body systems. For Bell inequalities with more than two outcomes, Jordan’s lemma [55], which ensures that the maximal quantum violation (Tsirelson bound) is attained with qubits, no longer applies. Therefore, higher dimensional systems, such as qutrits, may be necessary to saturate its maximal quantum expectation value. Already for relatively simple Bell inequalities in bipartite scenarios, unbounded Hilbert space dimensions may be required to reach the Tsirelson bound [56]. This fact prompts us to use our Bell inequality as a dimension witness of the underlying single-particle Hilbert space. To this end, one needs to compute its bound over the set of dimension-constrained quantum correlations. This problem was first considered in Ref. [57]. Later, Refs. [58, 59] characterized this set via convex optimization techniques by adding suitable dimension constraints to the celebrated Navascués-Pironio-Acín hierarchy [60]. However, the increasing computa-

tional complexity of these approaches makes it unfeasible to implement them for more than a few parties. In the present work, we exploit the symmetries of the proposed Bell inequality to provide a scalable relaxation of these dimensionality bounds, which results in practical witnesses for single-particle dimensionality of many-body quantum correlations.

Three-outcome Bell inequalities are also naturally fitted to explore the role of nonlocal correlations in three-level many-body systems, such as paradigmatic three-level models [61, 62] or spin-1 atomic ensembles [63, 64]. For instance, one may consider spin-1 Bose-Einstein condensates routinely implemented in the lab using  $^{87}\text{Rb}$  atoms [65, 66], where quantum correlations among the particles appears in the form of spin-nematic squeezing Ref. [67]. In this work, we explore the certification of Bell correlations and genuine three-level many-body correlations in such class of systems via collective measurements.

This paper is organized as follows. In Section II we provide an introduction to Bell nonlocality in the multipartite scenario and present the specific permutation-invariant Bell inequality that we will characterize in this work. In Section III, we show the possibility of using the proposed inequality as a dimension witness for qutrits and we analyze the state that violates this criteria. In Section IV, we apply our criteria to various systems of physical interest, such as spin-nematic squeezed Bose-Einstein condensates, and we derive Bell correlation and Bell dimension witnesses tailored to such experiments. Finally, in Section V we summarize our results.

## II. PERMUTATION-INVARIANT BELL INEQUALITIES (PIBIS)

**Scenario.**— We consider a  $(n, k, r)$  Bell scenario, i.e  $n$  parties, each of them having access to  $m$  measurement settings with  $r$  outcomes, see Fig. 1. After several rounds of collecting results, they are able to infer one- and two-body marginal probability distributions

$$\vec{p} = \{p_i(a|x), p_{ij}(ab|xy)\}. \quad (1)$$

Here,  $p_i(a|x)$  is the probability for party  $i \in [n]$  to obtain outcome  $a \in [r]$  when measuring  $x \in [k]$ . Likewise,  $p_{ij}(ab|xy)$  is the conditional probability for parties  $(i, j)$  to obtain outcomes  $(a, b)$  by measuring  $(x, y)$ , respectively. In the following, we will refer to these marginal probability distributions or to other statistics that may be inferred from the experiment as *data*.

**Local-realistic correlations.**— The correlations Eq. (1) might admit a classical explanation, namely through the so-called local-hidden variable models (LHVMs). In such a case, up to shared randomness, the correlations factor-

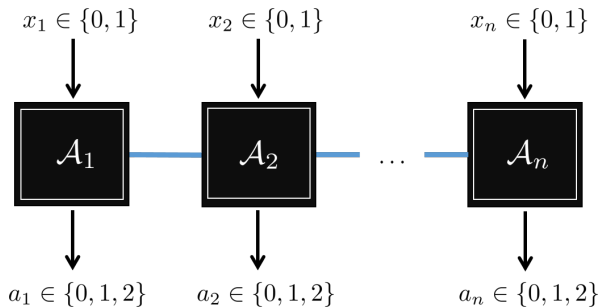


FIG. 1: Sketch of the  $(n, 2, 3)$  Bell scenario. Each party  $\mathcal{A}$  is represented as a *black box*, to highlight ignorance about its physical description. In every run of the experiment, each party  $i \in [n]$  independently chooses to perform measurement  $x_i$  on their share of the system and then register the resulting outcome  $a_i$ . After enough repetitions, the collected results can be used to infer the joint statistics, e.g. Eq. (1), from which quantum correlations can be detected.

ize as

$$p_{ij}(ab|xy) = \int_{\lambda \in \Lambda} p_i(a|x, \lambda) p_j(b|y, \lambda) d\mu(\lambda), \quad (2)$$

where  $\{d\mu(\lambda)\}_{\lambda \in \Lambda}$  is a probability measure. The set of probabilities  $\vec{p}$  may be interpreted as a real vector in an affine space. In such a geometric picture, the set of all LHV correlations forms a *polytope*  $\mathbb{P}$ , i.e. a convex set with finite number of vertices. This is delimited by linear inequalities of the form  $B = \vec{\alpha} \cdot \vec{p} - \beta_c \geq 0$ , namely *Bell inequalities* (BIs) with coefficients  $\vec{\alpha}$  and classical bound  $\beta_c$ . The minimal set of such inequalities describe the facets of  $\mathbb{P}$ . As BIs are necessarily fulfilled for any  $\vec{p}$  described by LHVMs, the violation of one of them signals *Bell nonlocality* or, in other words, the impossibility to explain the inferred statistics through LHVMs. If the data  $\vec{p}$  is derived from a quantum state via the Born rule, the violation of a BI also certifies quantum entanglement.

**Permutation invariance.**— In this work, we focus on families of BIs that are scalable in the number of parties  $n$ . To construct some of these, we impose symmetries in the Bell scenario [41, 50]. Specifically, we consider probabilities that are averaged over all permutations of the subsystems as

$$\begin{aligned} \mathcal{P}_{a|x} &= \sum_{i \in [n]} p_i(a|x) \\ \mathcal{P}_{ab|xy} &= \sum_{i \neq j \in [n]} p_{ij}(ab|xy). \end{aligned} \quad (3)$$

Note that we may refer this terms as probabilities, despite the fact that they have a different normalisation convention.

The local polytope  $\mathbb{P}$ , as defined earlier, is thus projected onto the space of permutation-invariant correlations Eq. (3). This projection is also a polytope,  $\mathbb{P}_S$ , which contains all the permutation-invariant (PI)

correlations admitting a LHV explanation. The exponential growth in the number of parties  $n$  of the dimension of  $\mathbb{P}$  deems our considered scenario intractable in the general case. However, the projection operation reduces drastically the combinatorial complexity of the problem and it allows for explicit construction of  $\mathbb{P}_S$  for a few parties  $n$ .

**Family of three-outcome PIBIs.**— To find Bell inequalities that hold for any  $n$ , a possible approach is to fully solve the local polytope  $\mathbb{P}_S$  for small  $n$ , and infer patterns in the coefficients of the inequalities [41, 52, 68]. Our goal is to do this in the  $(n, 2, 3)$  scenario, but the complexity of the problem does not allow us to go further than  $n = 3$ . We thus impose an additional symmetry, corresponding to an invariance under relabelling of inputs and outputs 0, 1 (see Appendix A). This allows us to fully solve the resulting polytope until  $n \sim 17$  with reasonable computational power. With this, we are able to identify the Bell inequality

$$B = \tilde{\mathcal{P}}_0 + \tilde{\mathcal{P}}_{00} - 2\tilde{\mathcal{P}}_{01} \geq 0, \quad (4)$$

where we have defined  $\tilde{\mathcal{P}}_0 := \mathcal{P}_{0|0} + \mathcal{P}_{0|1} + \mathcal{P}_{1|0} + \mathcal{P}_{1|1}$  corresponding to the symmetrized one-body term, and  $\tilde{\mathcal{P}}_{00} := \mathcal{P}_{00|00} + \mathcal{P}_{00|11} + \mathcal{P}_{11|00} + \mathcal{P}_{11|11}$ ,  $\tilde{\mathcal{P}}_{01} := \mathcal{P}_{01|01} + \mathcal{P}_{01|10}$ , corresponding to the symmetrized two-body terms. Note that outcome 2 does not appear explicitly, as it was eliminated using the normalization of probabilities. Eq. (4) represents a new family of *permutation-invariant Bell inequalities* (PIBIs). As for any other Bell inequality, violation of a PIBI certifies Bell nonlocality. For details on the derivation of Eq. (4) we refer the reader to Appendix A, where we also verify that  $B \geq 0$  is a *tight* PIBI for arbitrary number of parties  $n$ .

**Bell nonlocality versus Bell correlation.**— In the multipartite scenario, the cost to infer the values Eq. (1) increases exponentially with the number of parties  $n$ . However, under some reasonable assumptions, the coarse-grained statistics presented in Eq. (3) can be inferred in a scalable manner from collective observables only. Such assumptions include the validity of quantum mechanics, an accurate calibration of the measurements, or trusting that the parties are not communicating through unknown channels. In such a case, since we do not follow the strict prescriptions of a Bell experiment, we can no longer claim the detection of Bell nonlocality. Instead, we use the term *Bell correlations* to denote the violation of witnesses constructed from BIs assuming quantum mechanics, and which can be based on collective observables [43]. Through these witnesses, Bell correlations have been detected successfully in spinor Bose-Einstein condensates (BECs) experiments [43] and in cold atomic ensembles [44]. Bell correlations can be detected also in spin chains [69–72] from full-body correlations [48, 49]. Refinement of these witnesses enabled a more robust detection [52, 68], and the characterization

of such correlations through entanglement depth [20] or Bell correlation depth [21]. In this work, we aim at constructing similar Bell correlation witnesses from three-outcome PIBIs, and use them to certify the local dimension of many-body states.

### III. SCALABLE BELL DIMENSION WITNESS

The central contribution of this work is to demonstrate the use of PIBIs as *dimension witnesses*, which are able to certify the local Hilbert space's dimension of the underlying many-body state. When considering Bell inequalities with two dichotomic measurements per party, Jordan lemma ensures their maximal violation can already be achieved by qubits [55]. However, for three (or more) outcomes, such as in the case of Eq. (4), higher dimensional states may be necessary to reach a certain amount of violation. In such a case, the expectation value of the Bell operator gives a lower bound for the dimension of the local Hilbert space.

**Quantum correlations.**– For the remainder of this work, we will assume the data Eq. (2) to have a quantum description. In doing so, we associate a local Hilbert space  $\mathcal{H}$  to each party, thus expecting that the observed correlations originate from a global quantum state  $\hat{\rho}$  on the composite system  $\mathcal{H}^{\otimes n}$  according to Born's rule

$$\begin{aligned} p_i(a|x) &= \text{Tr}[\hat{\pi}_{a|x}(i)\hat{\rho}] := \langle \hat{\pi}_{a|x}(i) \rangle \\ p_{ij}(ab|xy) &= \text{Tr}[\hat{\pi}_{a|x}(i)\hat{\pi}_{b|y}(j)\hat{\rho}] := \langle \hat{\pi}_{a|x}(i)\hat{\pi}_{b|y}(j) \rangle. \end{aligned} \quad (5)$$

Here,  $\{\hat{\pi}_{a|x}\}_{a \in [r]}$  are generic positive-operator valued measures (POVMs) and the notation  $\hat{\pi}_{a|x}(i)$  indicates the application of operator  $\hat{\pi}_{a|x}$  on party  $i$  with trivial action in the remaining parties.

**Bell operator.**– Within the quantum framework, the Bell inequality value  $B$  is recovered as expectation value of the Bell operator  $\hat{\mathcal{B}}$ ,  $B = \langle \hat{\mathcal{B}} \rangle$ . Due to PI symmetry of the Bell inequality, the Bell operator is expressed in terms of collective operators only, namely operators taking the form  $\hat{O} = \sum_{i \in [n]} \hat{o}(i)$ , where  $\hat{o}(i)$  acts non-trivially only on party  $i \in [n]$ . Such operators are constructed from the individual POVM elements as

$$\left\{ \hat{\Pi}_{a|x} = \sum_{i \in [n]} \hat{\pi}_{a|x}(i) \right\}. \quad (6)$$

The Bell operator corresponding to PIBI Eq. (4) is then written as

$$\hat{\mathcal{B}} = \underbrace{(\hat{\Pi}_{0|0} - \hat{\Pi}_{1|1})^2 + (\hat{\Pi}_{0|1} - \hat{\Pi}_{1|0})^2}_{:=\hat{\mathcal{B}}_2} + \underbrace{\sum_{i \in [n]} \hat{\beta}(i)}_{\hat{\mathcal{B}}_1}, \quad (7)$$

where we denoted by  $\hat{\mathcal{B}}_2$  the quadratic term, which includes two-body all-to-all correlations, and by  $\hat{\mathcal{B}}_1$  the remaining collective term. Each addend in  $\hat{\mathcal{B}}_1$  is of the form

$$\hat{\beta} = \hat{\pi}_{0|0} + \hat{\pi}_{1|1} - (\hat{\pi}_{0|0} - \hat{\pi}_{1|1})^2 + \hat{\pi}_{0|1} + \hat{\pi}_{1|0} - (\hat{\pi}_{0|1} - \hat{\pi}_{1|0})^2. \quad (8)$$

The derivation of Eq. (7) can be found in Appendix B. Expressing the Bell operator in collective linear,  $\hat{\mathcal{B}}_1$ , and quadratic,  $\hat{\mathcal{B}}_2$ , terms, highlights the possibility of using collective measurements to probe PIBI Eq. (4) as a Bell correlation witness. As expected, Eq. (7) may be inferred from the local measurements  $\{\hat{\pi}_{a|x}\}$  in the standard Bell scenario, but also from average of the collective measurements  $\hat{\mathcal{B}}_1$  and second moments (i.e. fluctuations) of  $(\hat{\Pi}_{0|0} - \hat{\Pi}_{1|1})$ ,  $(\hat{\Pi}_{0|1} - \hat{\Pi}_{1|0})$  to probe for Bell correlation.

**Dimension witness.**– In order to derive dimension witnesses, we need to build inequalities fulfilled by any  $n$ -partite state of local dimension  $d = \dim(\mathcal{H})$ . To this end, we take the Bell operator for PIBI Eq. (4) and find a lower bound to its expectation value over all single-party POVMs on a  $n$ -qudit quantum states. Then, if for any certain measurement settings on a many-body quantum state we find that such bound is surpassed, one can conclude the corresponding data cannot be explained by  $n$  qudits. This implies that at least one of the subsystems needs to have a dimension greater than  $d$ . Unfortunately, the optimization problem leading to such a bound is outside standard computational capabilities already for few particles  $n$ . Moreover, convexity is not guaranteed. In the following, we propose a relaxation of this problem that is scalable in the number of parties, even more, its complexity does not grow with this parameter.

**Scalable dimension bound.**– As mentioned above, the derivation of a dimensionality-constrained bound to a BI is in general extremely demanding in the multipartite setting. However, the structure of the Bell operator Eq. (7) enables a scalable relaxation of such a bound. Indeed, we notice that the quadratic part is positive semidefinite (PSD),  $\langle \hat{\mathcal{B}}_2 \rangle \geq 0$ . This observation implies that it is sufficient to bound the linear term  $\langle \hat{\mathcal{B}}_1 \rangle$ , which leaves us with a single-party problem. Suppose that for a qudit of dimension  $d$ , the single-party term cannot surpass  $\beta_d$ ,  $\langle \hat{\beta} \rangle_d \geq \beta_d$ . Then,

$$\langle \hat{\mathcal{B}} \rangle \geq n\beta_d, \quad (9)$$

is a proper Bell dimension witness for arbitrary number of subsystems  $n$ . Regardless of the nature of the measurement settings  $\{x\}$  and without relying on trust in their implementation, if the inferred statistics violate Eq. (9) one must conclude that qudits of dimension  $d$  are insufficient to model the experiment and that at least one subsystem has dimension greater than  $d$ . Note that Eq. (9)



can be generalized to certify the dimension of  $n' > 1$  subsystems. Indeed, if  $\langle \hat{\mathcal{B}} \rangle < (n + 1 - n')\beta_d + (n' - 1)\beta_\infty$ , where  $\beta_\infty$  is the minimal value of  $\langle \hat{\mathcal{B}} \rangle$  for any Hilbert space dimension, then at least  $n'$  subsystems must have dimension greater than  $d$ .

The optimization of the local term  $\langle \hat{\beta} \rangle$  is much simpler than bounding the full Bell operator  $\langle \hat{\mathcal{B}} \rangle$ . In the next subsection, we elaborate on how to determine the bound  $\beta_d$ . In particular, we formulate PIBI Eq. (4) as a multi-qutrit witness, i.e. a witness that if violated signals that at least one subsystem is not a qubit. Moreover, beyond Eq. (7), our relaxation can be applied to any PI Bell operator with non-negative collective quadratic term. For instance, when it is decomposed as a sum of squares of collective operators, as in Eq. (7). Many classes of useful PIBIs follow this form [50].

### A. Evaluation of the dimension-constrained bound

The local operator  $\hat{\beta}$  Eq. (8) can be interpreted as a polynomial  $p$  of degree two in the non-commuting variables corresponding to the measurement operators  $\hat{\pi} = \{\hat{\pi}_{a|x}\}$ , namely  $\beta = p(\hat{\pi})$ . The optimization that we have to tackle is a dimension-constrained polynomial optimization problem

$$\beta_d := \min_{\substack{\hat{\pi}, |\psi\rangle \in \mathbb{C}^d \\ \text{s.t.}}} \frac{\langle \psi | p(\hat{\pi}) | \psi \rangle}{\hat{\pi}_{a|x} \succeq 0, \sum_a \hat{\pi}_{a|x} = \mathbb{1}} \quad (10)$$

This class of problems have been studied extensively in the past, also to bound BIs over dimension constraints [58, 59]. However, to the best of our knowledge, none of these previous works are applicable to multipartite scenarios because of the exponential scaling of the number of correlators to be considered. Here, we highlight how solving a single-party version of such problem may be sufficient to derive useful Bell dimension witnesses.

The polynomial  $p(\hat{\pi})$  still contains quadratic terms, which makes its optimization nontrivial and prompt us to resort to numerical methods. In the following, we propose two approaches to evaluate bound Eq. (10), and apply them to PIBI Eq. (4) for  $d = 2$  (qubits).

#### 1. Variational approach

The first approach we propose is variational, meaning that we directly express the problem Eq. (10) as the following unconstrained optimization. First, we introduce a parametrization of the local  $r$ -outcome qudit POVMs  $\{\hat{\pi}_{a|x}(\theta)\}$  (see Appendix C). Then, we numerically minimize  $\langle 0 | p(\hat{\pi}) | 0 \rangle$  over  $\theta$  to obtain as a solution  $\tilde{\beta}_d \geq \beta_d$ . For the case of Eq. (8), the optimization gives  $\tilde{\beta}_2 = -1/4$  for qubits and  $\tilde{\beta}_3 = -1/2$  for qutrits.

In addition, the algorithm also returns the optimal measurement settings, which appear to be the projec-

tors  $\hat{\pi}_{a|x} = |a, x\rangle\langle a, x|$ . For  $d = 2$ , after a suitable local unitary transformation, we can bring setting  $x = 0$  to the computational basis,  $\{\hat{\pi}_{0|0} = |0\rangle\langle 0|, \hat{\pi}_{1|0} = 0, \hat{\pi}_{2|0} = |2\rangle\langle 2|\}$ . Then, the optimal measurement  $x = 1$  is described by

$$\begin{aligned} |0, 1\rangle &= 0 \\ |1, 1\rangle &= \frac{\sqrt{3}}{2} |0\rangle - \frac{1}{2} |2\rangle \\ |2, 1\rangle &= \frac{1}{2} |0\rangle + \frac{\sqrt{3}}{2} |2\rangle. \end{aligned} \quad (11)$$

Notice that both measurement settings are effectively two-level, as they act only on  $\{|0\rangle, |2\rangle\}$ , c.f. Section IV A.

For  $d = 3$ , as done above, we can write setting  $x = 0$  in the computational basis,  $\{\hat{\pi}_{0|0} = |0\rangle\langle 0|, \hat{\pi}_{1|0} = |1\rangle\langle 1|, \hat{\pi}_{2|0} = |2\rangle\langle 2|\}$ , which results in the optimal measurement  $x = 1$  to be

$$\begin{aligned} |0, 1\rangle &= \frac{1}{2} |0\rangle + \frac{1}{2} |1\rangle + \frac{1}{\sqrt{2}} |2\rangle \\ |1, 1\rangle &= \frac{1}{2} |0\rangle + \frac{1}{2} |1\rangle - \frac{1}{\sqrt{2}} |2\rangle \\ |2, 1\rangle &= \frac{1}{\sqrt{2}} |0\rangle - \frac{1}{\sqrt{2}} |1\rangle. \end{aligned} \quad (12)$$

Consider that  $\{|0\rangle, |1\rangle, |2\rangle\}$  have well-defined spin-1 along the  $z$  direction,  $\hat{s}_z$  (see Appendix E for its explicit representation), corresponding to  $\{1, -1, 0\}$  respectively. Then, the states  $\{|0, 1\rangle, |1, 1\rangle, |2, 1\rangle\}$  are eigenstates of the  $\hat{s}_x$  observable with eigenvalues  $\{1, -1, 0\}$ , respectively. Thus, one may use single-party spin-1 observables,  $\hat{s}_z$  and  $\hat{s}_x$ , to probe for Bell correlations and for their dimensionality with PIBI Eq. (4), c.f. Section IV B.

The problem Eq. (10) addressed with the variational approach is not convex. This fact implies that the solver may converge to a local minimum, resulting in an overestimation of the bound,  $\tilde{\beta}_d \geq \beta_d$ . Such overestimation is prohibitive, as qubit systems could violate the associated dimensionality witness for the measurement settings of the global minimum. In order to certify its value, one thus needs to approach the bound  $\beta_d$  from below. To this end, we will adapt a convex relaxation of the problem based on hierarchies of semidefinite programs (SDPs) [73], which are a class of well-behaved optimization problems efficiently solved by available routines [74].

#### 2. Semidefinite programming approach

The second approach we propose consists in relaxing the minimization Eq. (10) with a sequence of SDPs. We outline here the method and its results, leaving technical details on its implementation in Appendix C.

The starting point consists of treating the measurement settings  $\hat{\pi}$  as noncommuting symbols. Then, we

assemble these and their products up to a certain order  $l$  in a list,  $\hat{\mathbf{m}} = \{1, \hat{\pi}, \hat{\pi}^2, \dots, \hat{\pi}^l\}$ , where e.g.  $\hat{\pi}^2$  contains all the degree 2 monomials, including  $\hat{\pi}_{0|0}^2, \hat{\pi}_{0|0}\hat{\pi}_{11}$ , etc. This list of monomials serves as basis to construct the moment matrix  $\Gamma = \langle \hat{\mathbf{m}}^\dagger \hat{\mathbf{m}} \rangle$ , which constitutes the central object of this approach. In this way, each entry of  $\Gamma$  corresponds to the expectation value of a monomial. Note that, by construction, the moment matrix is Hermitian,  $\Gamma = \Gamma^\dagger$ , and positive semidefinite,  $\Gamma \succeq 0$ . The objective function  $\langle p(\hat{\pi}) \rangle$  can now be expressed as a linear combination of the entries of  $\Gamma$ , namely as  $\langle p(\hat{\pi}) \rangle = \text{Tr}(C\Gamma)$  with  $C$  a matrix of real coefficients. Similarly, the PSD constraints  $\{\hat{\pi}_{a|x} \succeq 0, \sum_a \hat{\pi}_{a|x} = \mathbb{1}\}$  are translated into linear matrix inequalities  $\Lambda(\Gamma) \succeq 0$ , with  $\Lambda$  the corresponding (hermiticity-preserving) linear map. Thus, the problem we want to solve takes now the form

$$\min_{\Gamma \succeq 0} \quad \text{Tr}(C\Gamma) \\ \text{s.t.} \quad \Lambda(\Gamma) \succeq 0, \quad (13)$$

which is a SDP.

Note that, in the problem Eq. (13) we have not yet introduced the parameter  $d$ , that is, the local Hilbert space dimension is still unspecified. Consequentially, the resulting value will lower bound  $\beta_\infty$ , and the inequality  $\langle \hat{\mathcal{B}} \rangle \geq n\beta_\infty$  will be necessarily fulfilled for any data with a quantum explanation. This can be understood as a single-particle relaxation of the NPA algorithm introduced in Ref. [60] to approximate the Tsirelson bound. We evaluate the bound for our example PIBI Eq. (4) and obtain  $\beta = -1/2$ , which coincides with the qutrit bound presented in the previous paragraph. Such a bound can also be recovered analytically (see Appendix C).

The next step involves introducing the constraints on the local Hilbert space dimension. For this, several strategies has been proposed in the literature, such as the use of matrix polynomial identities or sampling methods [58]. Here we follow the latter: we sample qudit POVMs for a specific  $d$  and a state  $\rho$ , compute the corresponding moment matrix  $\Delta_1$ . We do so until a basis of moment matrices  $\{\Delta_i\}$  feasible by qudit data is completed. Then, the constraint  $\Gamma = \sum_i f_i \Delta_i$ , with  $\{f_i\}$  free real coefficients, restricts  $\Gamma$  onto the intersection of the PSD cone with the subspace of dimensionality constrained data. By applying such method to the PIBI Eq. (4) for qubits  $d = 2$ , we recover the variational bound  $\beta = -1/4$  at level  $l = 3$  of the SDP hierarchy.

The relaxation proposed here gives a rigorous bound. However, it is potentially more memory demanding than the variational approaches. In fact, as the dimension  $d$  is increased a higher level  $l$  must be considered.

From the previous discussion, we conclude that for any data originating from an  $n$ -qubit system, the Bell inequality shifted by the qubit bound (cf. Eq. (9))

$$B = \tilde{\mathcal{P}}_0 + \tilde{\mathcal{P}}_{00} - 2\tilde{\mathcal{P}}_{01} \geq -n/4 \quad (14)$$

holds. Therefore, if such inequality is violated, one can

certify that higher dimensional states (e.g. qutrits) are necessary to describe the inferred correlations.

## B. Comparison of the bounds

We close this section by comparing the scalable bound for qubits and for qutrits with the Bell expectation value that can be realized exactly by the optimal settings returned from the variational optimization Eqs. (11,12).

The Bell operator associated to PIBI Eq. (4) can be expressed as

$$\hat{\mathcal{B}} = \hat{T}_0 + \hat{T}_1^2 + \hat{T}_2^2, \quad (15)$$

for  $\{\hat{T}_a = \sum_{i \in [N]} \hat{t}_a^{(i)}\}$  certain collective operators [c.f. Eq. (7)]. If the optimal measurements are chosen, the single-particle operators for the qubit case read

$$\begin{aligned} \hat{t}_0 &= -(1/4) |0\rangle\langle 0| + (3/4) |1\rangle\langle 1| + 2 |2\rangle\langle 2| \\ \hat{t}_1 &= (\sqrt{3}/2) |0\rangle\langle 1| + \text{h.c.} \\ \hat{t}_2 &= 0, \end{aligned} \quad (16)$$

and for qutrit

$$\begin{aligned} \hat{t}_0 &= -(1/2) |0\rangle\langle 0| + |1\rangle\langle 1| + (1/2) |2\rangle\langle 2| \\ \hat{t}_1 &= |0\rangle\langle 1| + \text{h.c.} \\ \hat{t}_2 &= (1/\sqrt{2}) |0\rangle\langle 2| + \text{h.c.} \end{aligned} \quad (17)$$

where, for simplicity, we have written them in the basis  $\{|0\rangle, |1\rangle, |2\rangle\}$  where  $\hat{t}_0$  is diagonal.

We then represent the Bell operator Eq. (15) in the totally symmetric subspace of  $n$  qutrits. Such subspace is of dimension  $\binom{n+2}{2} = (n+2)(n+1)/2$  and it is spanned by the qutrit Dicke states [75]

$$|S_\mu\rangle = \binom{n}{\mu}^{-1/2} \sum_{\pi \in \mathfrak{S}_n} \pi \left( |0\rangle^{\otimes \mu_0} |1\rangle^{\otimes \mu_1} |2\rangle^{\otimes \mu_2} \right), \quad (18)$$

where  $\mu = (\mu_0, \mu_1, \mu_2)$  is a partition of  $n$ , i.e. a set of integers adding up to  $n$ ,  $\mu_0 + \mu_1 + \mu_2 = n$ ,  $\binom{n}{\mu} = n! / (\mu_0! \mu_1! \mu_2!)$  is the multinomial coefficient, and the sum is over distinct permutations  $\pi \in \mathfrak{S}_n$ . In physical terms,  $\{\mu_0, \mu_1, \mu_2\}$  represent the occupation number onto levels  $\{|0\rangle, |1\rangle, |2\rangle\}$ , respectively. Since the total number of particle is fixed, we take  $\mu_0, \mu_1$  to be the independent variables describing the state and set  $\mu_2 = n - \mu_0 - \mu_1$ .

We now probe the minimal eigenvalue of the Bell operator,  $\lambda_{\min}(\hat{\mathcal{B}})$ , for different number of parties  $n$ . If  $\hat{\mathcal{B}}$  is interpreted as a Hamiltonian [76],  $\lambda_{\min}(\hat{\mathcal{B}})$  is its ground state energy. The results are shown in Fig. 2 (blue dots for qubit and orange stars for qutrit). In the same Figure, we also display an analytical approximation of the previous minimal eigenvalues (solid blue line for qubits and orange dashed line for qutrits), which become tight in the thermodynamic limit  $n \rightarrow \infty$ . These are

based on the Holstein-Primakoff (HP) mapping, which we outline below.

**Holstein-Primakoff mapping.**— From the structure of the Bell operator Eq. (15), in order to minimize its expectation value one has to minimize the mean value of  $\hat{T}_0$  while minimizing the fluctuations (second moments) of  $\hat{T}_1$  and  $\hat{T}_2$  as well. Notice that the ground state of  $\hat{T}_0$  corresponds to all parties occupying state  $|0\rangle$ , i.e.  $|0\rangle^{\otimes n} = |S_{(n,0,0)}\rangle$  as “the winner takes it all”. For large system sizes, the effect of  $\hat{T}_1, \hat{T}_2$  can be treated perturbatively. To this end, we consider  $|S_{(n,0,0)}\rangle$  as the vacuum of a two-mode oscillator with creation operators  $a_1^\dagger, a_2^\dagger$ , exciting parties from  $|0\rangle$  to  $|1\rangle$  and  $|2\rangle$ , respectively [76]. With this ansatz, one can linearize  $\hat{\mathcal{B}}$  and obtain an analytical expression for the ground energy (see Appendix D for the derivation)

$$E_2 = -\frac{n}{4} + \frac{1}{2}(\sqrt{3n+1} - 1)$$

$$E_3 = -\frac{n}{2} - \frac{5}{4} + \sqrt{\frac{3n}{2} + \left(\frac{3}{4}\right)^2} + \sqrt{\frac{n}{2} + \left(\frac{1}{2}\right)^2}. \quad (19)$$

In such a limit,  $n \gg 1$ , the optimal settings for  $\langle \hat{\beta} \rangle$  converge to the optimal settings for the full Bell operator. As a consequence, Eqs. (19) are to be understood as finite size corrections to the scalable bounds addressed in the previous subsection. As a byproduct of this calculation, we verify that in the thermodynamic limit the (tight) quantum bound of PIBI Eq. (4) is indeed  $-n/2$ , and that it can be saturated by qutrits. The measurements considered here lose their optimality for small system sizes. Such finite-size effect can be appreciated in Fig. 2, where notice qubit states with stronger violation than qutrit.

Having established the bounds, we now move to characterize further the states that maximally violate PIBI Eq. (4), or its associated Bell dimension witness Eq. (9). In particular, we notice from Fig. 2 that qutrit states surpass the qubit bound when  $n \gtrsim 54$ , which signals the detection of correlations that cannot result from qubit states. In the following we give an example of such a genuine three-level Bell nonlocal state.

**Gaussian superposition of qutrit Dicke states.**— We illustrate in Fig. 3 the totally symmetric ground state  $|\Psi\rangle$  of the qutrit Bell operator for  $n = 15$ , by plotting its coefficients with respect the Dicke basis Eq. (18) after a suitable local rotation.

From Fig. 3, we can appreciate how the state  $|\Psi\rangle$  has non-vanishing support in all three levels and how it is almost invariant under their permutation. Such observations support the fact that it is genuinely three-level. Interestingly, this state can be approximated analytically by a Gaussian superposition of qutrit states centered at

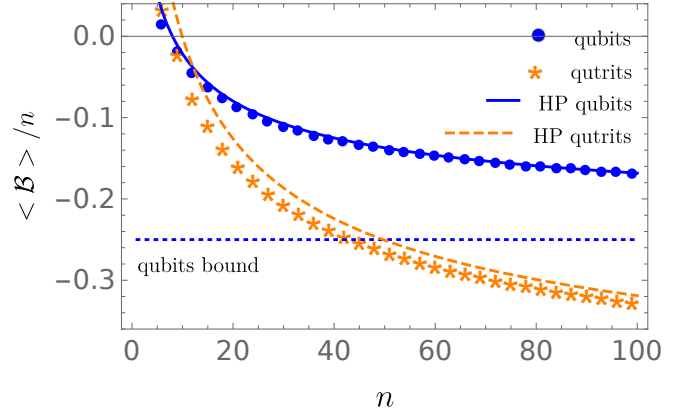


FIG. 2: Bounds on the Bell expectation value as a function of the number of parties  $n$ . Any expectation value below the classical bound (zero, thin black line) imply Bell nonlocality. The blue dots represent the minimal Bell expectation value reachable by performing on totally symmetric states of qubit the optimal settings specified in Eq. (11). The orange stars are the minimal Bell expectation value from measurements Eq. (12) performed on totally symmetric states of qutrit. Finally, the dotted horizontal line (blue) indicates the scalable qubit bound derived in Eq. (9).

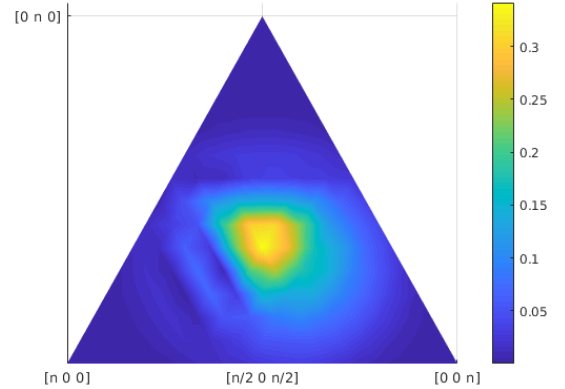


FIG. 3: Visualization of the state  $|\Psi\rangle$  maximally violating Bell operator Eq. (15) with optimal qutrit settings Eq. (12) and  $n = 15$  parties. The color scale indicates the overlap with the Dicke basis  $|\langle \Psi | S_n \rangle|$ .

the balanced Dicke state  $|S_{(n/3, n/3, n/3)}\rangle$ , namely as

$$\langle \Psi | S_\mu \rangle \approx \mathcal{N} \exp \left\{ -\frac{1}{2} \begin{pmatrix} \mu_0 - \frac{n}{3} \\ \mu_1 - \frac{n}{3} \end{pmatrix} \Sigma^{-1} \begin{pmatrix} \mu_0 - \frac{n}{3} & \mu_1 - \frac{n}{3} \end{pmatrix} \right\} \quad (20)$$

where  $\mathcal{N}$  is the normalization constant and  $\Sigma = s \begin{pmatrix} 1 & 1/2 \\ 1/2 & 1 \end{pmatrix}^{-1}$  is the covariance matrix of the distribution with  $s$  characterizing its width. Similar states can be found in spin-1/2 Lipkin models in equilibrium conditions [77], or in ground states of spin-1 condensates [78]. Inspired by this, we will illustrate in the next section the

usefulness of PIBI Eq. (4) and dimension witness Eq. (14) to detect and characterize nonlocal correlations in physically relevant many-body states.

#### IV. APPLICATIONS

Let us consider a system composed by a number  $n$  of three-level parties, that is, a collection of  $n$  qutrits. As it turns out, many properties of qubit systems (i.e. spins) are lost in higher dimensions. Here we mention two of them. First, qubit transformations can be understood as rotations, since the  $SU(2)$  Lie group is the double cover of the special orthogonal group  $SO(3)$ . Second, in  $SU(2)$  there is only one invariant function of its generators, i.e. one Casimir element; namely the total spin. On the other hand,  $SU(3)$  has two Casimir operators, which has consequences for quantum chaos [62] and spin squeezing [79]. For these (and other) reasons, three-level systems are fundamentally different and much richer than their two-level counterparts.

**Structure of  $\mathfrak{su}(3)$  algebra.**— The fundamental representation of  $\mathfrak{su}(3)$ , describing three-level local degrees of freedom  $\{|0\rangle, |1\rangle, |2\rangle\}$ , is given by the eight Gell Mann matrices  $\{\hat{\lambda}_a\}$  (see Appendix E). In particular,  $\{\hat{\lambda}_0, \hat{\lambda}_1, \hat{\lambda}_2\}$  constitutes a canonical representative of a  $\mathfrak{su}(2)$  subalgebra, as this triad satisfies the spin-1/2 commutation relations  $[\hat{\lambda}_a, \hat{\lambda}_b] = 2i\epsilon_{abc}\hat{\lambda}_c$ , where  $\epsilon_{abc}$  is the Levi-Civita symbol. Following Ref. [79], we denote this subspace as *type-2*. A second spin-1/2 subalgebra, the so-called *type-1*, is generated by the spin-1 (or dipole) matrices  $\{\hat{s}_x, \hat{s}_y, \hat{s}_z\}$ . This triad can be completed to a basis of  $\mathfrak{su}(3)$  by taking certain components of the nematic (or quadrupole) tensor  $\hat{q}_{ab} = \hat{s}_a\hat{s}_b/2 + \text{h.c.}$  (see Appendix E for an explicit representation). In this context, type-2 subspaces can also be written using spin and nematic components, for this reason, they are often called spin-nematic. As a matter of fact, type-1 and type-2 are the only unitarily inequivalent  $\mathfrak{su}(2)$  subalgebras of  $\mathfrak{su}(3)$  [79]. To any of these observables, we associate the corresponding collective operators, e.g.  $\hat{S}_x = \sum_{i \in [n]} \hat{s}_x^{(i)}$ ,  $\hat{Q}_{zz} = \sum_{i \in [n]} \hat{q}_{zz}^{(i)}$  etc., which we denote by upper-case letters. Note that these satisfy the same algebra as their single-party counterparts.

**Experimental implementation.**— Multilevel collective measurements are routinely implemented in atomic ensembles, such as in spinor (i.e. multicomponent) Bose Einstein condensates (BECs) [63, 64]. There, the population in each atomic level is usually resolved by splitting the BEC components through an external magnetic field, to then count the number of particles by absorption imaging [80]. This effectively corresponds to a Stern-Gerlach-type experiment, which realizes a projective measurement in the  $\hat{S}_z$  basis. To measure along any other basis, it is possible to implement unitary transformation that

bring the desired basis onto  $\hat{S}_z$  [81]. In the concrete, this is implemented experimentally in e.g. alkali-atom hyperfine spin states by rf-pulses and quadratic Zeeman energy shifts [67, 82]. We refer the reader to Appendix E for further details.

##### A. Detecting pseudospin squeezing

In this first illustration we consider effective two-level projective measurements to test our BIs. We assume all parties have access to the same two measurement settings, both belonging to the type-2 subalgebra spanned by  $\{\hat{\lambda}_0, \hat{\lambda}_1, \hat{\lambda}_2\}$ . Then, without loss of generality, we can consider both measurements to lie on  $\{\hat{\lambda}_0, \hat{\lambda}_1\}$  plane with an angle  $2\theta$  between each other, namely

$$\begin{aligned}\hat{m}_0 &= \cos(\theta)\hat{\lambda}_0 + \sin(\theta)\hat{\lambda}_1 \\ \hat{m}_1 &= \cos(\theta)\hat{\lambda}_0 - \sin(\theta)\hat{\lambda}_1.\end{aligned}\quad (21)$$

The corresponding projectors are  $\{\hat{\pi}_+ = (1 + \hat{m})/2, \hat{\pi}_- = (1 - \hat{m})/2, \hat{\pi}_\circ = |2\rangle\langle 2|\}$ , and we associate them to the three outputs  $\{0, 1, 2\}$  of the PIBI as  $\{+, \circ, -\}$  for measurement 0 and  $\{\circ, -, +\}$  for measurement 1. In this scenario, the expectation value of the Bell operator Eq. (7) can be written as a function of  $\theta$  and of the data

$$\begin{aligned}x &:= \langle \hat{\Lambda}_0^2 \rangle / (n - \langle \hat{n}_2 \rangle) \\ y &:= \langle \hat{\Lambda}_1 \rangle / (n - \langle \hat{n}_2 \rangle) \\ z &:= (n - \langle \hat{n}_2 \rangle) / n,\end{aligned}\quad (22)$$

where  $\hat{\Lambda}_a = \sum_{i \in [n]} \lambda_a(i)$  are the collective Gell-Mann matrices and  $\hat{n}_2 = \sum_{i \in [n]} |2\rangle\langle 2|(i)$  represents the occupation number of level 2. Minimization of  $\langle \hat{\mathcal{B}} \rangle$  over  $\theta$  allows us to write  $\langle \hat{\mathcal{B}} \rangle \geq 0$  as the Bell correlation witness

$$2x + \sqrt{\frac{(z-2)^2}{z^2} - y^2} + \frac{2}{z} - 3 \geq 0. \quad (23)$$

Details on the derivation of this result can be found in Appendix F. Violation of Eq. (23) reveals Bell nonlocality if the statistics  $\{x, y, z\}$  are inferred from a proper Bell scenario, or Bell correlation otherwise.

Let us analyze now the features of the states violating such an inequality. For  $z$  constant, RHS of Eq. (23) is minimized if  $x$  (i.e.  $\langle \hat{\Lambda}_0^2 \rangle$ ) is minimal while  $y$  (i.e.  $|\langle \hat{\Lambda}_1 \rangle|$ ) is maximal. States with large mean value of  $\hat{\Lambda}_1$  and reduced fluctuations of  $\hat{\Lambda}_0$  are pseudospin squeezed states. Such class of many-body states display high sensitivity for rotations generated by  $\Lambda_3$  and thus find application in quantum metrology [83]. Their entanglement content has also been characterized extensively [84–87]. One of the most celebrated entanglement witness for spin squeezing is the Wineland criterion [88, 89], which can be rewritten following the notation introduced in Eq. (22) as

$$\frac{4}{z} - \frac{y^2}{x} \geq 0. \quad (24)$$



Let us now focus on the population measurement  $z$ . The optimal case (to achieve maximal violation) is when the whole system occupy the two pseudospin levels, so that  $\langle \hat{n}_2 \rangle = 0$  (or  $z = 1$ ). Then, Eq. (23) becomes the Bell correlation witness for a 2-outcome PIBI of Ref. [43]. Thus, the new witness we propose can be seen as a generalization to three levels of a known Bell correlation witness. We envision this to be relevant for open systems or imperfect detection, as the third outcome could represent e.g. particle losses or inconclusive measurements. Note that if the number of particles fluctuates from one experimental round to the next, it is possible to introduce the total number operator  $\hat{n}$  and replace e.g.  $x$  by  $\langle \hat{\Lambda}_0^2 / (\hat{n} - \hat{n}_2) \rangle$ . This is due to the fact that number and pseudospin operators commute, see Ref. [43].

Even if the witness we have proposed is tailored to three-level systems, the use of effective two-level measurements (type-2) makes it ineffective for dimensionality certification. Indeed, the qubit bound Eq. (10) can never be violated for this choice of measurements. In fact, computing the maximal Bell violation for the proposed measurement settings will never violate  $\langle \hat{B} \rangle \geq -n/4$  and in the thermodynamic limit  $n \rightarrow \infty$ , the ideal pseudospin-squeezed state saturates such bound. Nonetheless, the witness Eq. (23) is applicable to detect Bell correlation. We illustrate it below for squeezed states prepared in a spin-1 BECs.

**Spin nematic squeezing in BECs.**— We consider a BEC of  $n$  spin-1 atoms with contact interactions subject to an external magnetic field of intensity  $B$ . In the so-called single mode approximation, the Hamiltonian of the system reads [64, 67]

$$\hat{H} = \frac{c}{2n} \hat{\mathbf{S}}^2 + g \hat{Q}_{zz}, \quad (25)$$

where  $\hat{\mathbf{S}} = \sum_{i \in [n]} \hat{\mathbf{s}}^{(i)}$  is the collective spin-1 operator,  $\hat{Q}_{zz}$  is the collective quadrupole operator,  $c$  is the interaction strength and  $g \sim B^2$  represents the quadratic Zeemann shift.

As demonstrated in Ref. [67], the spin-mixing dynamics governed by Hamiltonian Eq. (23) induces pseudospin (or spin-nematic) squeezing. In particular, starting from the polar state  $|0\rangle^{\otimes n}$ , pseudospin squeezing will develop in the type-2 subspace generated by  $\{\hat{S}_x, 2\hat{Q}_{yz}, \hat{Q}_{zz} - \hat{Q}_{yy}\}$ . To illustrate the detection of Bell correlation in spin-nematic squeezed BEC states, we consider  $n = 30$  atoms,  $c = -1 < 0$  (simulating  $^{87}\text{Rb}$ ) and  $g = 0.2$ . We evolve the polar state  $|0\rangle^{\otimes n}$  according to Hamiltonian Eq. (25) for time  $t$ , which results in  $|\Psi(t)\rangle = e^{-it\hat{H}} |0\rangle^{\otimes n}$ . For each preparation time  $t$ , we compute the mean values  $\langle \hat{Q}_{zz} + \hat{Q}_{yy} \rangle$ ,  $\langle \hat{Q}_{zz} - \hat{Q}_{xx} + \hat{Q}_{yy} \rangle$  and the fluctuations (second moments)  $\{\langle \hat{S}_x^2 \rangle, \langle \hat{Q}_{yz}^2 \rangle, \langle \hat{S}_x \hat{Q}_{yz} + \text{h.c.} \rangle\}$ . Such statistics is sufficient to infer the optimal data corresponding to the squeezed fluctuations  $x$ , mean (pseudo)spin  $y$  and population  $z$  entering the witness Eq. (23). See Appendix F for details on the derivation.

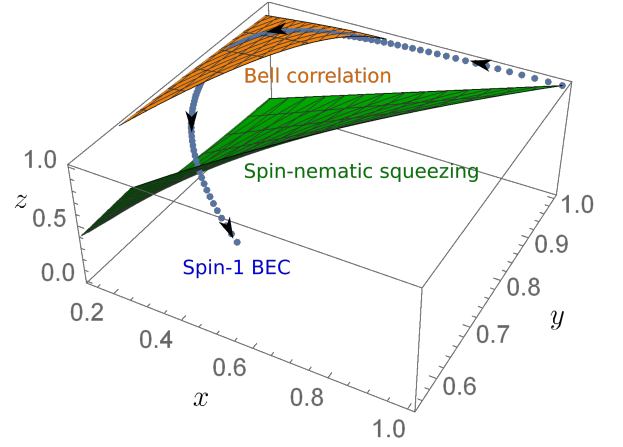


FIG. 4: Comparison of the spin-nematic witness Eq. (24) (green surface) and the Bell correlation witness Eq. (23) (orange surface). Data above such surfaces indicates a violation of the corresponding witness. The blue dots represent the data obtained from evolving a polar state  $|0\rangle^{\otimes n}$  of  $n = 30$  spin-1 particles according to Hamiltonian Eq. (25).

The results of our numerical simulation are shown in Fig. 4. The time-evolution dynamics is plotted as blue points in the  $xyz$ -space, together with the surfaces representing the Bell correlation witness Eq. (23) (orange) and the Wineland entanglement criterion Eq. (24) (green). At  $t = 0$ , the polar state  $|0\rangle^{\otimes n}$  appears in the top-right corner, with coordinates  $(x, y, z) = (1, 1, 1)$ . As time progresses,  $x$  is reduced, i.e. spin-nematic squeezing is generated. This results very quickly in the violation of Eq. (24), which signals entanglement among the particles in the systems. For longer evolution times the correlations get so strong that Eq. (23) is also violated, indicating the presence of Bell correlations. Ultimately, even longer evolution times results in over-squeezed states with small polarizations (reduced first moments of the collective spin), for which the considered witnesses are inadequate to detect correlations.

## B. Detecting genuine three-level correlations

For the next illustration, we will consider instead spin-1 projections. As before, we assume all parties have access to the same two measurement settings, both belonging to the type-1 subalgebra spanned by  $\{\hat{s}_x, \hat{s}_y, \hat{s}_z\}$ . Then, without loss of generality, we can consider both measurements to lie on  $\{\hat{s}_x, \hat{s}_y\}$  plane with an angle  $2\theta$  between each other, namely

$$\begin{aligned} \hat{m}_0 &= \cos(\theta) \hat{s}_x + \sin(\theta) \hat{s}_y \\ \hat{m}_1 &= \cos(\theta) \hat{s}_x - \sin(\theta) \hat{s}_y. \end{aligned} \quad (26)$$

We associate output 0 with the projector onto spin projection +1 and likewise output 1 for spin -1 for both measurements, i.e.,  $a \in [2]$ ,  $\hat{\pi}_{0|a} = (\hat{m}_a^2 + \hat{m}_a)/2$ ,  $\hat{\pi}_{1|a} =$

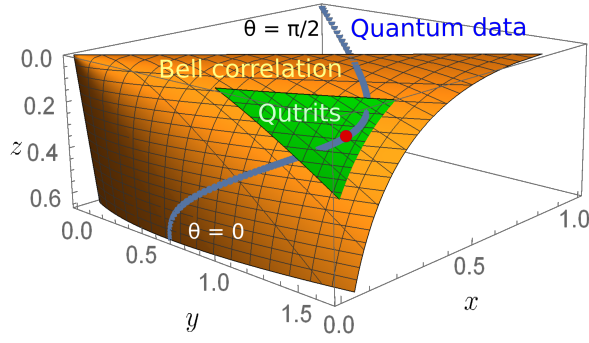


FIG. 5: Comparison of the dimension witness Eq. (28) for  $\beta = 0$  (orange surface) and  $\beta = -1/4$  (green surface). Data above such surfaces indicates a violation of the corresponding witness. In the specific, data above the orange surface signals Bell correlation while data above the green surface reflects expectation values that cannot be reproduced by multi-qubit systems. The blue dots represent the data obtained from the minimal eigenvalue of  $\hat{\mathcal{B}}(\theta)$  at uniform intervals of  $\theta \in [0, \pi/2]$ . The red dot represents the expectation values for  $\theta = \pi/4$ .

$(\hat{m}_a^2 - \hat{m}_a)/2$ . Considering this choice of settings, the Bell operator  $\hat{\mathcal{B}}$  is a function of  $\theta$  and of the data  $(x, y, z)$  that we redefine here as

$$\begin{aligned} x &= \langle \hat{S}_x^2 \rangle / n \\ y &= \langle 3\hat{Q}_{zz} + \hat{Q}_{xx} - 8\hat{Q}_{xy}^2 - 2n\mathbb{I} \rangle / n \\ z &= \langle \hat{Q}_{yy} \rangle / n \end{aligned} \quad (27)$$

As before, we minimize the Bell expectation value  $\langle \hat{\mathcal{B}}(\theta) \rangle$  over  $\theta$ , which results now in the witness

$$x - \frac{1}{2}(y + 3z) + \sqrt{2x(y + z) - \beta(y + z)} \geq 0, \quad (28)$$

where  $\beta$  is the considered bound, i.e.  $\langle \hat{\mathcal{B}} \rangle \geq n\beta$ . For  $\beta = 0$ , Eq. (28) serves as a Bell correlation witness. On the other hand, for  $\beta = -1/4$  it serves as a Bell dimension witness for qutrits. If the latter is violated, it indicates that at least one subsystem has dimension greater than two. The derivation of Eq. (28) can be found in Appendix G.

In Fig. 5 we illustrate as surfaces in the  $xyz$ -space the witnesses obtained from Eq. (28) for  $\beta = 0$  (orange) and  $\beta = -1/2$  (green). In addition, we plot the data derived from the minimal eigenvector of  $\hat{\mathcal{B}}(\theta)$  for a range of angles  $\theta \in (0, \pi/2)$  and  $n = 60$  parties. These states deliver maximal violation. Crucially, for some values of  $\theta$  the qubit bound is violated, indicating presence of genuine three-level Bell correlations. The strongest violation is achieved for  $\theta = \pi/4$  (red dot), which results in an eigenstate equivalent to the one discussed in Fig. 3, or to the ground state of Bell operator Eq. (15) with qutrit settings Eq. (17). We shall complete this subsection by addressing the squeezing properties of such states.

**SU(3) squeezing.**— In the previous subsection we have seen that spin-squeezed states violate the most the Bell correlation witness for qubit states Eq. (23). This behaviour is similar here: States showing strong violation possess large mean value of  $\langle \hat{T}_0 \rangle$ , which plays the role of mean spin polarization generalized to three-level systems. However, now the fluctuations along  $\hat{T}_1, \hat{T}_2$  are simultaneously suppressed. That is, both pseudospin spaces  $\{|0\rangle, |1\rangle\}$  and  $\{|0\rangle, |2\rangle\}$  appear squeezed at the same time. Hence, these states could be useful for multiparameter estimation tasks [90, 91]. Finally, the impossibility of representing these correlations with qubits directly arises from the fact that the two pseudospin subspaces are not independent, which indicates quantum resources with high dimensionality.

## V. CONCLUSIONS

In this work, we have presented a scalable permutationally invariant Bell inequality based on one- and two-body correlation functions of three-outcome measurements. Such a Bell inequality is suited to probe nonlocality in three-level (or spin-1) system of arbitrary number of particles, since it can be converted into a Bell correlation witness that depends on experimentally accessible collective observables.

From a modification of this witness, we propose a method to derive Bell dimension witnesses, namely criteria that signal the impossibility of a given statistics to originate from measurements on an  $n$ -body state of some single-particle Hilbert space dimension  $d$ . The method we propose is based on computing scalable bounds to the maximal violation achievable with dimension-constrained single-particle Hilbert spaces. In particular, we focus on the qubit case,  $d = 2$ , and characterize physically relevant statistics violating the corresponding dimension witness. These include e.g. Gaussian superpositions of qutrit Dicke states that can appear as ground states of SU(3) Hamiltonians [61, 62]. Beyond the specific inequality addressed in this work, our method can be applied to other multi-level multipartite Bell inequalities that have been proposed in the past [50].

Next, we verify that the states maximally violating the criteria we proposed are experimentally relevant. In particular, we find that our Bell correlation witness detects nonlocality in spin-nematic squeezed states, as the one demonstrated in spin-1 Bose Einstein condensates [67]. However, despite the fact that these correlations originate in spin-1 systems, they can effectively be described by qubits [92]. In this sense, the simple spin-nematic squeezing we have considered does not lead to a violation of the Bell dimension witness. We show that states that do violate the dimension witness, and thus are certified to be genuine three-level nonlocal, correspond to SU(3) states where two effective qubit subspaces appear simultaneously squeezed. These states could still be prepared in spin-1 BECs through more complicated nonlinear dy-

namics [91] and could be exploited for multiparameter estimation protocols [90].

In summary, our work paves the way to detect Bell correlations in multipartite spin-1 systems and to use many-outcome Bell inequalities as dimension witnesses. These can be adopted experimentally to certify the single-party dimension of many-body quantum states and the presence of high-dimensional nlocal correlations.

**Code and data availability.**— The code and data to construct the plots are available at the following link [https://github.com/GuillemMRR/3-PIBIs\\_dimW](https://github.com/GuillemMRR/3-PIBIs_dimW).

**Acknowledgments.**— We thank Irénée Frérot for useful discussions.

GM and ML acknowledge support from: Europea Research Council AdG NOQIA; MCIN/AEI (PGC2018-0910.13039/501100011033, CEX2019-000910-S/10.13039/501100011033, Plan National FIDEUA PID2019-106901GB-I00, Plan National STAMEENA PID2022-139099NB, I00, project funded by MCIN/AEI/10.13039/501100011033 and by the “European Union NextGenerationEU/PRTR” (PRTR-C17.I1), FPI); QUANTERA MAQS PCI2019-111828-2); QUANTERA DYNAMITE PCI2022-132919, QuantERA II Programme co-funded by European Union’s Horizon 2020 program under Grant Agreement No 101017733); Ministry for Digital Transformation and of Civil Service of the Spanish Government through the QUANTUM ENIA project call - Quantum Spain project, and by the European Union through the Recovery, Transformation and Resilience Plan - NextGenerationEU within the framework of the Digital Spain 2026 Agenda; Fundació Cellex; Fundació Mir-Puig; Generalitat de Catalunya (European Social Fund FEDER and CERCA program, AGAUR Grant No. 2021 SGR 01452, QuantumCAT U16-011424, co-funded by ERDF Operational Program of Catalonia 2014-2020); Barcelona Supercomputing Center MareNostrum (FI-2023-3-0024); Funded by

the European Union. Views and opinions expressed are however those of the author(s) only and do not necessarily reflect those of the European Union, European Commission, European Climate, Infrastructure and Environment Executive Agency (CINEA), or any other granting authority. Neither the European Union nor any granting authority can be held responsible for them (HORIZON-CL4-2022-QUANTUM-02-SGA PASQuanS2.1, 101113690, EU Horizon 2020 FET-OPEN OPTologic, Grant No 899794), EU Horizon Europe Program (This project has received funding from the European Union’s Horizon Europe research and innovation program under grant agreement No 101080086 NeQSTGrant Agreement 101080086 — NeQST); ICFO Internal “QuantumGaudi” project; European Union’s Horizon 2020 program under the Marie Skłodowska-Curie grant agreement No 847648; “La Caixa” Junior Leaders fellowships, La Caixa” Foundation (ID 100010434); CF/BQ/PR23/11980043.

AA acknowledges support from the Austrian Science Fund (FWF) (projects P 33730-N and 10.55776/PAT2839723) and by the ESQ Discovery programme (Erwin Schrödinger Center for Quantum Science & Technology), hosted by the Austrian Academy of Sciences (ÖAW).

MF was supported by the Swiss National Science Foundation Ambizione Grant No. 208886, and The Branco Weiss Fellowship – Society in Science, administered by the ETH Zürich.

JT has received support from the European Union’s Horizon Europe program through the ERC StG FINE-TEA-SQUAD (Grant No. 101040729). JT also acknowledges support from the Quantum Delta NL program. This publication is part of the ‘Quantum Inspire – the Dutch Quantum Computer in the Cloud’ project (with project number [NWA.1292.19.194]) of the NWA research program ‘Research on Routes by Consortia (ORC)’, which is funded by the Netherlands Organization for Scientific Research (NWO).

- 
- [1] A. Einstein, B. Podolsky, and N. Rosen, *Phys. Rev.* **47**, 777 (1935).
  - [2] J. S. Bell, *Physics* **1**, 195 (1964).
  - [3] N. Brunner, D. Cavalcanti, S. Pironio, V. Scarani, and S. Wehner, *Rev. Mod. Phys.* **86**, 419 (2014).
  - [4] M. Pawłowski, T. Paterek, D. Kaszlikowski, V. Scarani, A. Winter, and M. Żukowski, *Nature* **461**, 1101 EP (2009).
  - [5] T. Fritz, A. B. Sainz, R. Augusiak, J. B. Brask, R. Chaves, A. Leverrier, and A. Acín, *Nature Communications* **4**, 2263 EP (2013), article.
  - [6] M. Navascués, Y. Guryanova, M. J. Hoban, and A. Acín, *Nature Communications* **6**, 6288 EP (2015), article.
  - [7] L. Lydersen, C. Wiechers, C. Wittmann, D. Elser, J. Skaar, and V. Makarov, *Nature Photonics* **4**, 686 EP (2010).
  - [8] A. Acín, N. Brunner, N. Gisin, S. Massar, S. Pironio, and V. Scarani, *Phys. Rev. Lett.* **98**, 230501 (2007).
  - [9] D. Mayers and A. Yao, *Quantum Information & Computation* **4**, 273 (2004).
  - [10] A. Salavrakos, R. Augusiak, J. Tura, P. Wittek, A. Acín, and S. Pironio, *Phys. Rev. Lett.* **119**, 040402 (2017).
  - [11] J. Wang, S. Paesani, Y. Ding, R. Santagati, P. Skrzypczyk, A. Salavrakos, J. Tura, R. Augusiak, L. Mančinska, D. Bacco, D. Bonneau, J. W. Silverstone, Q. Gong, A. Acín, K. Rottwitt, L. K. Oxenløwe, J. L. O’Brien, A. Laing, and M. G. Thompson, *Science* **360**, 285 (2018).
  - [12] J. Kaniewski, I. Supic, J. Tura, F. Baccari, A. Salavrakos, and R. Augusiak, <http://arxiv.org/abs/1807.03332v1>.
  - [13] R. Colbeck and R. Renner, *Nature Physics* **8**, 450 EP (2012).

- [14] I. Šupić, R. Augusiak, A. Salavrakos, and A. Acín, *New Journal of Physics* **18**, 035013 (2016).
- [15] R. Arnon-Friedman, F. Dupuis, O. Fawzi, R. Renner, and T. Vidick, *Nature Communications* **9** (2018), 10.1038/s41467-017-02307-4.
- [16] J.-D. Bancal, N. Brunner, N. Gisin, and Y.-C. Liang, *Physical review letters* **106**, 020405 (2011).
- [17] T. Moroder, J.-D. Bancal, Y.-C. Liang, M. Hofmann, and O. Gühne, *Physical review letters* **111**, 030501 (2013).
- [18] Y.-C. Liang, D. Rosset, J.-D. Bancal, G. Pütz, T. J. Barnea, and N. Gisin, *Phys. Rev. Lett.* **114**, 190401 (2015).
- [19] F. Baccari, D. Cavalcanti, P. Wittek, and A. Acín, *Phys. Rev. X* **7**, 021042 (2017).
- [20] A. Aloy, J. Tura, F. Baccari, A. Acín, M. Lewenstein, and R. Augusiak, *Physical Review Letters* **123** (2019), 10.1103/physrevlett.123.100507.
- [21] F. Baccari, J. Tura, M. Fadel, A. Aloy, J.-D. Bancal, N. Sangouard, M. Lewenstein, A. Acín, and R. Augusiak, *Physical Review A* **100** (2019).
- [22] I. H. Deutsch, *PRX Quantum* **1**, 020101 (2020).
- [23] I. Frérot, M. Fadel, and M. Lewenstein, *Reports on Progress in Physics* **86**, 114001 (2023).
- [24] I. Pitowsky, *Quantum Probability — Quantum Logic*, Lecture Notes in Physics (Springer-Verlag, 1989).
- [25] L. Babai, L. Fortnow, and C. Lund, *Computational Complexity* **1**, 3 (1991).
- [26] I. Pitowsky and K. Svozil, *Physical Review A* **64**, 014102 (2001).
- [27] C. Śliwa, *Physics Letters A* **317**, 165 (2003).
- [28] S. Pironio, *Journal of Physics A: Mathematical and Theoretical* **47**, 424020 (2014).
- [29] O. Gühne, G. Tóth, P. Hyllus, and H. J. Briegel, *Phys. Rev. Lett.* **95**, 120405 (2005).
- [30] G. Tóth, O. Gühne, and H. J. Briegel, *Phys. Rev. A* **73**, 022303 (2006).
- [31] O. Gühne, G. Tóth, P. Hyllus, and H. J. Briegel, *Physical Review Letters* **95** (2005), 10.1103/physrevlett.95.120405.
- [32] F. Baccari, R. Augusiak, I. Šupić, J. Tura, and A. Acín, <http://arxiv.org/abs/1812.10428v1>.
- [33] J.-D. Bancal, N. Gisin, and S. Pironio, *Journal of Physics A: Mathematical and Theoretical* **43**, 385303 (2010).
- [34] J.-D. Bancal, C. Branciard, N. Brunner, N. Gisin, and Y.-C. Liang, *Journal of Physics A: Mathematical and Theoretical* **45**, 125301 (2012).
- [35] E. G. Cavalcanti, C. J. Foster, M. D. Reid, and P. D. Drummond, *Phys. Rev. Lett.* **99**, 210405 (2007).
- [36] Q. Y. He, E. G. Cavalcanti, M. D. Reid, and P. D. Drummond, *Phys. Rev. A* **81**, 062106 (2010).
- [37] C. Bamps and S. Pironio, *Physical Review A* **91** (2015), 10.1103/physreva.91.052111.
- [38] T. H. Yang and M. Navascués, *Physical Review A* **87** (2013), 10.1103/physreva.87.050102.
- [39] A. Coladangelo, K. T. Goh, and V. Scarani, *Nature Communications* **8**, 15485 EP (2017), article.
- [40] R. Augusiak, M. Demianowicz, M. Pawłowski, J. Tura, and A. Acín, *Physical Review A* **90** (2014), 10.1103/physreva.90.052323.
- [41] J. Tura, R. Augusiak, A. B. Sainz, T. Vértesi, M. Lewenstein, and A. Acín, *Science* **344**, 1256 (2014).
- [42] J. Tura, R. Augusiak, A. Sainz, B. Lücke, C. Klempt, M. Lewenstein, and A. Acín, *Annals of Physics* **362**, 370 (2015).
- [43] R. Schmied, J.-D. Bancal, B. Allard, M. Fadel, V. Scarani, P. Treutlein, and N. Sangouard, *Science* **352**, 441 (2016).
- [44] N. J. Engelsen, R. Krishnakumar, O. Hosten, and M. A. Kasevich, *Phys. Rev. Lett.* **118**, 140401 (2017).
- [45] A. Piga, A. Aloy, M. Lewenstein, and I. Frérot, *Physical Review Letters* **123** (2019).
- [46] F. Fröwis, M. Fadel, P. Treutlein, N. Gisin, and N. Brunner, *Physical Review A* **99** (2019), 10.1103/physreva.99.040101.
- [47] M. Fadel and J. Tura, *Phys. Rev. Lett.* **119**, 230402 (2017).
- [48] J. Chwedeńczuk, *SciPost Phys. Core* **5**, 025 (2022).
- [49] A. Niezgoda, M. Panfil, and J. Chwedeńczuk, *Phys. Rev. A* **102**, 042206 (2020).
- [50] G. Müller-Rigat, A. Aloy, M. Lewenstein, and I. Frérot, *PRX Quantum* **2**, 030329 (2021).
- [51] Z. Wang, S. Singh, and M. Navascués, *Phys. Rev. Lett.* **118**, 230401 (2017).
- [52] J. Guo, J. Tura, Q. He, and M. Fadel, *Phys. Rev. Lett.* **131**, 070201 (2023).
- [53] D. Collins, N. Gisin, N. Linden, S. Massar, and S. Popescu, *Physical Review Letters* **88** (2002), 10.1103/physrevlett.88.040404.
- [54] D. Alsina, A. Cervera, D. Goyeneche, J. I. Latorre, and K. Życzkowski, *Physical Review A* **94**, 032102 (2016).
- [55] C. Jordan, *Bulletin de la Société Mathématique de France* **3**, 103 (1875).
- [56] K. F. Pál and T. Vértesi, *Physical Review A* **82** (2010), 10.1103/physreva.82.022116.
- [57] N. Brunner, S. Pironio, A. Acín, N. Gisin, A. A. Méthot, and V. Scarani, *Phys. Rev. Lett.* **100**, 210503 (2008).
- [58] M. Navascués and T. Vértesi, *Physical review letters* **115**, 020501 (2015).
- [59] M. Navascués, A. Feix, M. Araújo, and T. Vértesi, *Phys. Rev. A* **92**, 042117 (2015).
- [60] M. Navascués, S. Pironio, and A. Acín, *New Journal of Physics* **10**, 073013 (2008).
- [61] H. Lipkin, N. Meshkov, and A. Glick, *Nuclear Physics* **62**, 188 (1965).
- [62] S. Gnutzmann, F. Haake, and M. Kus, *Journal of Physics A: Mathematical and General* **33**, 143 (1999).
- [63] T.-L. Ho, *Phys. Rev. Lett.* **81**, 742 (1998).
- [64] C. K. Law, H. Pu, and N. P. Bigelow, *Phys. Rev. Lett.* **81**, 5257 (1998).
- [65] M. Barrett, J. Sauer, and M. Chapman, *Physical Review Letters* **87**, 010404 (2001).
- [66] H. Schmaljohann, M. Erhard, J. Kronjäger, M. Kottke, S. van Staa, L. Cacciapuoti, J. J. Arit, K. Bongs, and K. Sengstock, *Phys. Rev. Lett.* **92**, 040402 (2004).
- [67] C. D. Hamley, C. S. Gerving, T. M. Hoang, E. M. Bookjans, and M. S. Chapman, *Nature Physics* **8**, 305 (2012).
- [68] S. Wagner, R. Schmied, M. Fadel, P. Treutlein, N. Sangouard, and J.-D. Bancal, *Physical Review Letters* **119**, 170403 (2017).
- [69] M. Płodzień, M. Kościelski, E. Witkowska, and A. Sinatra, *Phys. Rev. A* **102**, 013328 (2020).
- [70] M. Płodzień, M. Lewenstein, E. Witkowska, and J. Chwedeńczuk, *Phys. Rev. Lett.* **129**, 250402 (2022).
- [71] M. Płodzień, T. Wasak, E. Witkowska, M. Lewenstein, and J. Chwedeńczuk, *Phys. Rev. Res.* **6**, 023050 (2024).



- [72] M. Płodzień, J. Chwedeńczuk, and M. Lewenstein, “Inherent quantum resources in the stationary spin chains,” (2024).
- [73] P. Skrzypczyk and D. Cavalcanti, *Semidefinite Programming in Quantum Information Science*, 2053-2563 (IOP Publishing, 2023).
- [74] “The MOSEK optimization software,” .
- [75] A. Aloy, M. Fadel, and J. Tura, *New Journal of Physics* **23**, 033026 (2021).
- [76] M. Fadel and J. Tura, *Quantum* **2**, 107 (2018).
- [77] C. Marconi, A. Riera-Campeny, A. Sanpera, and A. Aloy, *Phys. Rev. A* **105**, L060201 (2022).
- [78] O. E. Müstecaplıoğlu, M. Zhang, and L. You, *Phys. Rev. A* **66**, 033611 (2002).
- [79] E. Yukawa, M. Ueda, and K. Nemoto, *Phys. Rev. A* **88**, 033629 (2013).
- [80] M.-S. Chang, C. Hamley, M. Barrett, J. Sauer, K. Fortier, W. Zhang, L. You, and M. Chapman, *Physical review letters* **92**, 140403 (2004).
- [81] P. Giorda, P. Zanardi, and S. Lloyd, *Phys. Rev. A* **68**, 062320 (2003).
- [82] J. D. Sau, S. R. Leslie, M. L. Cohen, and D. M. Stamper-Kurn, *New Journal of Physics* **12**, 085011 (2010).
- [83] L. Pezzè, A. Smerzi, M. K. Oberthaler, R. Schmied, and P. Treutlein, *Reviews of Modern Physics* **90** (2018), 10.1103/revmodphys.90.035005.
- [84] G. Müller-Rigat, M. Lewenstein, and I. Frérot, *Quantum* **6**, 887 (2022).
- [85] G. Vitagliano, P. Hyllus, I. L. Egusquiza, and G. Tóth, *Physical Review Letters* **107** (2011), 10.1103/physrevlett.107.240502.
- [86] G. Müller-Rigat, A. K. Srivastava, S. Kurdzialek, G. Rajchel-Mieldzioć, M. Lewenstein, and I. Frérot, *Quantum* **7**, 1152 (2023).
- [87] I. Apellaniz, B. Lücke, J. Peise, C. Klempt, and G. Tóth, *New Journal of Physics* **17**, 083027 (2015).
- [88] D. J. Wineland, J. J. Bollinger, W. M. Itano, and D. J. Heinzen, *Physical Review A* **50**, 67 (1994).
- [89] A. Sørensen, L.-M. Duan, J. I. Cirac, and P. Zoller, *Nature* **409**, 63 (2001).
- [90] M. Fadel, B. Yadin, Y. Mao, T. Byrnes, and M. Gessner, *New Journal of Physics* **25**, 073006 (2023).
- [91] J. Cao, X. Li, T. Mao, W. Xu, and L. You, “Joint estimation of a two-phase spin rotation beyond classical limit,” (2023).
- [92] J. Kitzinger, X. Meng, M. Fadel, V. Ivannikov, K. Nemoto, W. J. Munro, and T. Byrnes, *Phys. Rev. A* **104**, 043323 (2021).
- [93] A. Fine, *Physical Review Letters* **48**, 291 (1982).
- [94] K. Fukuda, Institute for Operations Research, ETH-Zentrum, 91 (1997).
- [95] A. Aloy, G. Müller-Rigat, J. Tura, and M. Fadel, “Deriving three-outcome permutationally invariant bell inequalities,” (2024), [arXiv:2406.11792](https://arxiv.org/abs/2406.11792) .
- [96] A. Aloy, G. Müller-Rigat, M. Lewenstein, J. Tura, and M. Fadel, “Bell inequalities as a tool to probe quantum chaos,” (2024), [arXiv:2406.11791](https://arxiv.org/abs/2406.11791) .
- [97] A. Tavakoli, D. Rosset, and M.-O. Renou, *Physical Review Letters* **122** (2019), 10.1103/physrevlett.122.070501.

## Appendix A: Construction of the local polytope and derivation of PIBIs

We provide in this Appendix additional details on the derivation of permutationally invariant Bell inequalities (PIBIs), as well as of their classical bound.

**Local-deterministic strategies.**— According to Fine theorem [93], the polytope of classical correlations may be constructed from its extremal points, i.e. from local deterministic strategies (LDS). LDS are rules which assign to each measurement setting a deterministic outcome. In the generic scenario, the number of LDS grows exponentially with  $n$ . Conversely, if PI is exploited, these can be characterized only by a set of non-negative integers  $c_{\mathbf{r}}$ , indicating the number of parties which exhibit outcomes string  $\mathbf{r}$  when measuring  $[k]$ . Note  $c_{\mathbf{r}} \geq 0$  and  $\sum_{\mathbf{r}} c_{\mathbf{r}} = n$ . In particular, PI reduces the number of LDS from  $r^{kn}$  to  $\binom{n+r-1}{k-1} \sim \mathcal{O}((n+r-1)^{(k-1)}/(k-1)!)$ .

The collective probabilities defined in the main text decompose under LDS as

$$\begin{aligned} \mathcal{P}_{a|x} &= \sum_{\mathbf{r}:\mathbf{x}=a} c_{\mathbf{r}} \\ \mathcal{P}_{ab|xy} &= \sum_{\mathbf{r}:\mathbf{x}=a} c_{\mathbf{r}} \sum_{\mathbf{r}':\mathbf{x}=a} c_{\mathbf{r}'} - \sum_{\substack{\mathbf{r}:\mathbf{x}=a \\ \mathbf{r}:\mathbf{y}=b}} c_{\mathbf{r}}. \end{aligned} \quad (\text{A1})$$

For sufficiently small number of parties  $n$ , one is able to enumerate the vertices of the local polytope in the space of PI correlations  $\{\mathcal{P}_{a|x}, \mathcal{P}_{ab|xy}\}$ . The convex hull of the vertices defines the polytope. An equivalent description of such body is through intersection of half-planes, i.e. Bell inequalities. Switching between these two representations is a linear program, which is routinely solved via well-established algorithms [94].

**Symmetrization of inputs/outputs.**— In order to improve further the scalability of the vertex enumeration problem, we introduce an additional symmetrization over the inputs and outputs labels. In the  $(n, 2, 3)$  scenario, such simplification reduces the dimension of the correlation space to the five quantities

$$\begin{aligned} \tilde{\mathcal{P}}_0 &= \mathcal{P}_{0|0} + \mathcal{P}_{0|1} + \mathcal{P}_{1|0} + \mathcal{P}_{1|1} \\ \tilde{\mathcal{P}}_{00} &= \mathcal{P}_{00|00} + \mathcal{P}_{00|11} + \mathcal{P}_{11|00} + \mathcal{P}_{11|11} \\ \tilde{\mathcal{P}}_{10} &= \mathcal{P}_{00|01} + \mathcal{P}_{11|01} \\ \tilde{\mathcal{P}}_{11} &= \mathcal{P}_{01|00} + \mathcal{P}_{01|11} \\ \tilde{\mathcal{P}}_{01} &= \mathcal{P}_{01|01} + \mathcal{P}_{10|10} \end{aligned} \quad (\text{A2})$$

Note that we disregarded outcome 2 without loss of generality by virtue of the non-signaling principle and normalization of the marginals [95]. The symmetry considered here is motivated by the fact that input and outcome labelling is a free choice, and thus arbitrary.

We proceed to fully characterize PIBIs in this reduced space, where they can be parametrize by the coefficients

$\vec{\alpha} = (\alpha_0, \alpha_1, \alpha_2, \alpha_3, \alpha_4)$  and the classical bound  $\beta_c$  as

$$B = \alpha_0 \tilde{\mathcal{P}}_0 + \alpha_1 \tilde{\mathcal{P}}_{00} + \alpha_2 \tilde{\mathcal{P}}_{10} + \alpha_3 \tilde{\mathcal{P}}_{11} + \alpha_4 \tilde{\mathcal{P}}_{01} - \beta_c \geq 0. \quad (\text{A3})$$

Such coefficients are in general dependent on the number of particles  $n$ . It is thus postselect PIBIs with constant coefficients, suggesting scalable inequalities that could be valid for any  $n$ . Among the inequalities found by this method we identified

$$B = \tilde{\mathcal{P}}_0 + \tilde{\mathcal{P}}_{00} - 2\tilde{\mathcal{P}}_{01} \geq 0, \quad (\text{A4})$$

coming from  $\vec{\alpha} = (1, 1, 0, 0, -2)$  and  $\beta_c = 0$ , which is presented as Eq. (4) in the main text.

We point the reader to Ref. [95] for a pedagogic introduction to the characterization of such projected polytopes and for more PIBIs of the form Eq. (A3).

Remarkably, as we are going to prove in the following, inequality (A4) is a faced of the projected polytope for any  $n$ , and it is thus a tight PIBI.

**Classical bound of Eq. (A4).**— To prove that the classical bound is tight, it is sufficient to verify that it can be saturated by LDS. These are characterized by the number of parties which exhibit outcomes  $(a, b)$  while measuring  $(0, 1)$ , namely by  $\{c_{ab} \geq 0\}$  with  $\sum_{a,b \in [3]} c_{ab} = n$ . If we define  $\mathbf{c} = (c_{00}, c_{11}, c_{02}, c_{20}, c_{12}, c_{21})$  then, after subtracting  $2(c_{10} + c_{01}) \geq 0$ , we have

$$B_{\text{LDS}} \geq \mathbf{c}^T \underbrace{\begin{pmatrix} 2 & -2 & 1 & 1 & -1 & -1 \\ -2 & 2 & -1 & -1 & 1 & 1 \\ 1 & -1 & 1 & 0 & 0 & -1 \\ 1 & -1 & 0 & 1 & -1 & 0 \\ -1 & 1 & 0 & -1 & 1 & 0 \\ -1 & 1 & -1 & 0 & 0 & 1 \end{pmatrix}}_{:=\mathcal{I}_{\text{LDS}}} \mathbf{c}. \quad (\text{A5})$$

It is easy to verify that  $\mathcal{I}_{\text{LDS}}$  is positive-semidefinite (PSD), i.e.  $\mathcal{I}_{\text{LDS}} \succeq 0$ , therefore  $B_{\text{LDS}} \geq 0$ . In particular,  $c_{22} = n$  gives  $B_{\text{LDS}} = 0$ , which completes the proof. An alternative proof can be found in Ref. [96].

## Appendix B: Derivation of the Bell operator for Eq. (4)

The collective quantities defined in Eq. (3) of the main text become in the collective picture

$$\begin{aligned} \mathcal{P}_{a|x} &= \langle \hat{\Pi}_{a|x} \rangle \\ \mathcal{P}_{ab|xy} &= \langle \{\hat{\Pi}_{a|x}, \hat{\Pi}_{b|y}\} - \hat{\Pi}_{ab|xy} \rangle, \end{aligned} \quad (\text{B1})$$

where,

$$\begin{aligned} \hat{\Pi}_{a|x} &= \sum_{i \in [n]} \hat{\pi}_i(a|x) \\ \hat{\Pi}_{ab|xy} &= \sum_{i \in [n]} \{\hat{\pi}_i(a|x), \hat{\pi}_i(b|y)\}, \end{aligned} \quad (\text{B2})$$

are collective operators and  $\{\cdot, \cdot\}$  is half the anticommutator. From these, we derive the symmetrized one and two-body terms

$$\begin{aligned}\tilde{\mathcal{P}}_0 &= \langle \hat{\Pi}_{0|0} + \hat{\Pi}_{0|1} + \hat{\Pi}_{1|0} + \hat{\Pi}_{1|1} \rangle \\ \tilde{\mathcal{P}}_{00} &= \langle \hat{\Pi}_{0|0}^2 - \hat{\Pi}_{00|00} + \hat{\Pi}_{0|1}^2 - \hat{\Pi}_{00|11} \\ &\quad + \hat{\Pi}_{1|0}^2 - \hat{\Pi}_{11|00} + \hat{\Pi}_{1|1}^2 - \hat{\Pi}_{11|11} \rangle \\ -2\tilde{\mathcal{P}}_{01} &= \langle \hat{\Pi}_{01|01} + \hat{\Pi}_{01|10} - \hat{\Pi}_{0|0}\hat{\Pi}_{1|1} \\ &\quad - \hat{\Pi}_{1|1}\hat{\Pi}_{0|0} - \hat{\Pi}_{0|1}\hat{\Pi}_{1|0} - \hat{\Pi}_{1|0}\hat{\Pi}_{0|1} \rangle.\end{aligned}\quad (\text{B3})$$

The sum of the LHS of the previous equations gives Eq. (4), while the RHS after completing the squares yields  $\langle \hat{\mathcal{B}} \rangle$  with  $\hat{\mathcal{B}}$  the Bell operator presented in Eq. (7). This is

$$\hat{\mathcal{B}} = (\hat{\Pi}_{0|0} - \hat{\Pi}_{1|1})^2 + (\hat{\Pi}_{0|1} - \hat{\Pi}_{1|0})^2 + \hat{\mathcal{B}}_1, \quad (\text{B4})$$

where,

$$\begin{aligned}\hat{\mathcal{B}}_1 &= \hat{\Pi}_{0|0} + \hat{\Pi}_{0|1} + \hat{\Pi}_{1|0} + \hat{\Pi}_{1|1} \\ &\quad - \hat{\Pi}_{00|00} - \hat{\Pi}_{00|11} - \hat{\Pi}_{11|00} - \hat{\Pi}_{11|11} \\ &\quad + 2(\hat{\Pi}_{01|01} + \hat{\Pi}_{01|10}).\end{aligned}\quad (\text{B5})$$

If the local measurements are projective,  $\hat{\pi}_{a|x}\hat{\pi}_{b|x} = \delta_{ab}\hat{\pi}_{b|x}$ , the one-body term further simplifies to

$$\hat{\mathcal{B}}_1 = 2(\hat{\Pi}_{01|01} + \hat{\Pi}_{01|10}). \quad (\text{B6})$$

### Appendix C: Derivation of dimension bounds for PIBI Eq. (4)

In this Appendix, we provide complementary details on the methods employed to find the qubit ( $d = 2$ ) bound to PIBI Eq. (4). We also comment on its generalization to  $d > 2$ .

**Variational.**— We parametrize the local  $r$ -outcome qudit POVMs in the extended Hilbert space  $\mathbb{C}^r \otimes \mathbb{C}^d$  via Naimark's dilation,

$$\hat{\pi}_{a|x} = \hat{P}_d e^{-i\theta_x \cdot \hat{\mathbf{G}}} |a\rangle\langle a|^{\otimes d} e^{i\theta_x \cdot \hat{\mathbf{G}}} \hat{P}_d, \quad (\text{C1})$$

where  $\hat{P}_d = \sum_{a \in [d]} |a\rangle\langle a|$  is a rank- $d$  projector,  $\theta_x \in \mathbb{R}^{(rd)^2-1}$  and  $\hat{\mathbf{G}}$  is a basis of traceless Hermitian operators acting in  $\mathbb{C}^r \otimes \mathbb{C}^d$ . We minimize  $\langle 0|p(\hat{\pi})|0\rangle$  over  $\{\theta_x\}_{x \in [k]}$  via a Nelder-Mead routine from `scipy.optimize.fmin`, which is specially suited for this nonconvex tasks.

**SDP relaxation.**— We take the single particle term,  $\langle \hat{\mathcal{B}}_1 \rangle$ , to be minimized over qubit POVMs. These satisfy  $\{\hat{\pi} \succeq 0\}$ ,  $\hat{\pi}_{0|0} + \hat{\pi}_{1|0} \preceq \mathbb{1}$  and  $\hat{\pi}_{0|1} + \hat{\pi}_{1|1} \preceq \mathbb{1}$ . As in Eq. (10), the problem consists of optimizing a polynomial of non-commuting variables. However, this problem is now constrained by the dimension of the local Hilbert

space. Since the Bell inequality is linear in the probabilities, extremal POVMs are sufficient. In the case of a qubit, those are of rank-1. As such, from Naimark dilation, they can be implemented in  $\mathbb{C}^3$  like  $\hat{\pi}_a = \hat{\mathbf{p}}\hat{\mathbf{t}}_a\hat{\mathbf{p}}$ , where  $\hat{\mathbf{p}}$  is a (fixed) rank-2 projector and  $\{\hat{\mathbf{t}}_a\}$  a rank-1 projective measurements,  $\hat{\mathbf{t}}_a\hat{\mathbf{t}}_b = \delta_{ab}\hat{\mathbf{t}}_b$ . We apply the Navascués-Vértesi hierarchy from the list of monomials  $\hat{\mathbf{m}} = (\mathbb{1}, \hat{\mathbf{p}}, \hat{\mathbf{t}}_{0|0}, \hat{\mathbf{t}}_{1|0}, \hat{\mathbf{t}}_{0|1}, \hat{\mathbf{t}}_{1|1})$  and sample random projectors to construct a basis of moment matrices  $\{\Delta_i\}$  feasible with qubit POVM. We solve the program with the commercially available package `qdimsum` based on Ref. [97]. At level 3 of the hierarchy we obtain the bound  $\beta_2 \geq -0.3091$ , while at level 4,  $\beta_2 \geq -0.2500$ .

If one disregards the dimension constraints, the above problem can be used to bound the Bell value over quantum correlations (for arbitrary dimension), i.e. its Tsirelson bound. By doing so, we get  $\beta_\infty \geq -0.5000$ . For completeness, we present here another proof of such bound. If the Hilbert space dimension remains unspecified, it is sufficient to consider local projective measurements,  $\hat{\pi}_{a|x}\hat{\pi}_{b|x} = \delta_{ab}\hat{\pi}_{b|x}$ . In such a case,

$$\hat{\beta} = 2(\langle \hat{\pi}_{0|0}, \hat{\pi}_{1|1} \rangle + \langle \hat{\pi}_{01}, \hat{\pi}_{10} \rangle), \quad (\text{C2})$$

which can be bounded as  $\langle \hat{\beta} \rangle \geq \langle (\hat{\pi}_{0|0} + \hat{\pi}_{1|1})(\hat{\pi}_{0|0} + \hat{\pi}_{1|1} - 1) + (\hat{\pi}_{0|1} + \hat{\pi}_{1|0})(\hat{\pi}_{0|1} + \hat{\pi}_{1|0} - 1) \rangle \geq \langle (\hat{\pi}_{0|0} + \hat{\pi}_{1|1}) \rangle \langle (\hat{\pi}_{0|0} + \hat{\pi}_{1|1} - 1) \rangle + \langle (\hat{\pi}_{0|1} + \hat{\pi}_{1|0}) \rangle \langle (\hat{\pi}_{0|1} + \hat{\pi}_{1|0} - 1) \rangle \geq -1/2$ , where we used  $\langle^2 \rangle \geq \langle \rangle^2$  and that  $0 \leq \langle \hat{\pi}_{a|x} \rangle \leq 1$  for all  $a, x \in \{0, 1\}$ .

### Appendix D: Holstein-Primakoff approximation

To illustrate the utility of the Holstein-Primakoff approximation, let us first discuss the qubit case,  $\text{SU}(2)$ . Consider the Hamiltonian

$$\hat{H} = c\hat{J}_x^2 + b\hat{J}_z, \quad (\text{D1})$$

where  $\hat{J}_x = \sum_{i \in [n]} (|0\rangle\langle 1| + \text{h.c.})^{(i)}/2$  and  $\hat{J}_z = \sum_{i \in [n]} (-|0\rangle\langle 0| + |1\rangle\langle 1|)^{(i)}/2$  are two collective spin components along orthogonal directions. As  $n \rightarrow \infty$ , the ground state (GS) of  $\hat{H}$  becomes almost fully polarized  $\langle \hat{J}_y \rangle = -n/2 + \delta$ , with  $\delta \ll 1$  for  $b \geq 0$ . We can treat this perturbation via Holstein-Primakoff spin-boson mapping [76], where the spin coherent state  $|0\rangle^{\otimes n}$  is interpreted as vacuum of the bosonic mode  $a$ . Then,  $\hat{J}_z \approx -n/2 + a^\dagger a$  and  $\hat{J}_x \approx \sqrt{n/4}(a^\dagger + a)$ . Hamiltonian Eq. (D1) is then rewritten as

$$H_{in} = -\frac{1}{2}b(n+1) + \frac{1}{2} \begin{pmatrix} a^\dagger & a \end{pmatrix} \begin{pmatrix} b + nc/2 & nc/2 \\ nc/2 & b + nc/2 \end{pmatrix} \begin{pmatrix} a \\ a^\dagger \end{pmatrix}. \quad (\text{D2})$$

We notice that it is quadratic in the bosonic modes, meaning it can be diagonalized analytically. To this end, we apply a Bogoliubov transformation  $a = \sqrt{(b + nc/2 + E)/(2E)}\gamma - \sqrt{(b + nc/2 - E)/(2E)}\gamma^\dagger$ , to bring it to the diagonal form  $H = E\gamma^\dagger\gamma + \text{const.}$  [76]. In

this case,  $E = \sqrt{(b + nc/2)^2 - (nc/2)^2}$  is the frequency of the oscillator. For the ground state,  $\langle \gamma^\dagger \gamma \rangle = 0$ . Consequently, its energy is given by the constant term

$$E_{GS} = -\frac{1}{2}b(n+1) + \frac{1}{2}\sqrt{(b + nc/2)^2 - (nc/2)^2}. \quad (\text{D3})$$

We notice that our Bell operator Eq. (15) is of the form Eq. (D1) up to a constant shift. Therefore, we can apply the steps just discussed, which yield  $E_2$  in Eq. (19).

The qutrit case is analogous. We interpret  $|0\rangle^{\otimes n}$  as the vacuum of two bosonic modes with creation operators  $a_1^\dagger, a_2^\dagger$  exciting particles from level  $|0\rangle$  to level  $|1\rangle$  and  $|2\rangle$  respectively. For sufficiently large system sizes, we can approximate  $\hat{T}_0 \approx (n - a_1^\dagger a_1 - a_2^\dagger a_2)/2 + a_1^\dagger a_1 + (1/2)a_2^\dagger a_2$  and  $\hat{T}_0 \approx \sqrt{n}(a_1^\dagger + a_1)$ ,  $\hat{T}_1 \approx \sqrt{n/2}(a_2^\dagger + a_2)$ . The corresponding linearized Hamiltonian reads

$$\begin{aligned} H_{\text{lin}} = & -\frac{n}{2} - \frac{5}{4} \\ & + (a_1^\dagger \ a_1) \begin{pmatrix} n+3/4 & n \\ n & n+3/4 \end{pmatrix} \begin{pmatrix} a_1 \\ a_1^\dagger \end{pmatrix} \\ & + \frac{1}{2} (a_2^\dagger \ a_2) \begin{pmatrix} n+1 & n \\ n & n+1 \end{pmatrix} \begin{pmatrix} a_2 \\ a_2^\dagger \end{pmatrix}. \end{aligned} \quad (\text{D4})$$

As before, we diagonalize this Hamiltonian by applying the appropriate Bogoliubov transformation in each mode, which yield  $E_3$  in Eq. (19).

### Appendix E: $\mathfrak{su}(3)$ matrices

We show the explicit matrix representations that we use for the Gell-Mann matrices and for the dipole-quadrupole spin-1 operators.

The representation of Gell-Mann matrices that we consider is

$$\begin{aligned} \lambda_0 &= \begin{pmatrix} 0 & 1 & 0 \\ 1 & 0 & 0 \\ 0 & 0 & 0 \end{pmatrix}, \lambda_1 = \begin{pmatrix} 0 & -i & 0 \\ i & 0 & 0 \\ 0 & 0 & 0 \end{pmatrix}, \\ \lambda_2 &= \begin{pmatrix} 1 & 0 & 0 \\ 0 & -1 & 0 \\ 0 & 0 & 0 \end{pmatrix}, \lambda_3 = \begin{pmatrix} 0 & 0 & 1 \\ 0 & 0 & 0 \\ 1 & 0 & 0 \end{pmatrix}, \\ \lambda_4 &= \begin{pmatrix} 0 & 0 & -i \\ 0 & 0 & 0 \\ i & 0 & 0 \end{pmatrix}, \lambda_5 = \begin{pmatrix} 0 & 0 & 0 \\ 0 & 0 & 1 \\ 0 & 1 & 0 \end{pmatrix}, \\ \lambda_6 &= \begin{pmatrix} 0 & 0 & 0 \\ 0 & 0 & -i \\ 0 & i & 0 \end{pmatrix}, \lambda_7 = \frac{1}{\sqrt{3}} \begin{pmatrix} 1 & 0 & 0 \\ 0 & 1 & 0 \\ 0 & 0 & -2 \end{pmatrix}. \end{aligned} \quad (\text{E1})$$

Let us note that the Gell-Mann matrices are normalized to a value of 2, *i.e.*,  $\text{tr}\{(\lambda_i \lambda_j)\} = 2\delta_{ij}$  with  $\delta_{ij}$  being the Kronecker delta.

The spin-1 dipole operators representation we consider

is

$$\begin{aligned} s_x &= \frac{1}{\sqrt{2}} \begin{pmatrix} 0 & 1 & 0 \\ 1 & 0 & 1 \\ 0 & 1 & 0 \end{pmatrix}, \\ s_y &= \frac{i}{\sqrt{2}} \begin{pmatrix} 0 & -1 & 0 \\ 1 & 0 & -1 \\ 0 & 1 & 0 \end{pmatrix}, \\ s_z &= \begin{pmatrix} 1 & 0 & 0 \\ 0 & 0 & 0 \\ 0 & 0 & -1 \end{pmatrix}, \end{aligned} \quad (\text{E2})$$

whose expectation values are components of the angular momentum vector. Finally, the spin-1 quadrupole operators representation we consider is

$$\begin{aligned} q_{yz} &= \frac{i}{2\sqrt{2}} \begin{pmatrix} 0 & -1 & 0 \\ 1 & 0 & 1 \\ 0 & -1 & 0 \end{pmatrix}, \\ q_{xz} &= \frac{1}{2\sqrt{2}} \begin{pmatrix} 0 & 1 & 0 \\ 1 & 0 & -1 \\ 0 & -1 & 0 \end{pmatrix}, \\ q_{xy} &= \frac{i}{2} \begin{pmatrix} 0 & 0 & -1 \\ 0 & 0 & 0 \\ 1 & 0 & 0 \end{pmatrix}, \\ q_{xx} &= \frac{1}{2} \begin{pmatrix} 1 & 0 & 1 \\ 0 & 2 & 0 \\ 1 & 0 & 1 \end{pmatrix}, \\ q_{yy} &= \frac{1}{2} \begin{pmatrix} 1 & 0 & -1 \\ 0 & 2 & 0 \\ -1 & 0 & 1 \end{pmatrix}, \\ q_{zz} &= \begin{pmatrix} 1 & 0 & 0 \\ 0 & 0 & 0 \\ 0 & 0 & 1 \end{pmatrix}, \end{aligned} \quad (\text{E3})$$

whose expectation values are moments of the symmetric quadrupole tensor. Note that out of the 6 quadrupole operators in Eq. (E3), only 5 of them are actually necessary to complete a basis. Therefore, in practice, one typically chooses to specify the linear combination  $q_{xx} - q_{yy}$  instead of the pair  $q_{xx}, q_{yy}$ .

**Experimental measurement of multilevel collective observables.**— Collective measurements of spin and quadrupole operators are routinely implemented in experiments with ultracold atomic ensembles through a Stern-Gerlach-type sequence. In fact, expectation values of physically observable spin operators can be expressed in terms of the populations in the three-levels for some appropriate basis. For example

$$\begin{aligned} \langle \hat{S}_x \rangle &= \langle \hat{n}_x^{(+1)} \rangle - \langle \hat{n}_x^{(-1)} \rangle \\ \langle \hat{Q}_{xx} \rangle &= \langle \hat{n}_x^{(+1)} \rangle + \langle \hat{n}_x^{(-1)} \rangle = n - \langle \hat{n}_x^{(0)} \rangle \\ \langle \hat{Q}_{xy} \rangle &= \langle \hat{n}_{(x+y)}^{(0)} / \sqrt{2} \rangle - \langle \hat{n}_{(x-y)}^{(0)} / \sqrt{2} \rangle \end{aligned} \quad (\text{E4})$$



Here,  $\langle \hat{n}_x^{(a)} \rangle$  represents the mean number of atoms in the hyperfine level  $a \in \{+1, 0, -1\}$  along basis  $x$ . Unfortunately, however, population measurements are always performed in the  $\hat{S}_z$  basis. Therefore, appropriate transformation need to be performed in order to rotate the desired basis onto the one for  $\hat{S}_z$ . This is conveniently done through rf-pulses and quadratic Zeeman shifts [67, 82].

### Appendix F: Bell correlation in pseudospin states

In this Appendix, we provide the derivation of the witnesses presented in subsection IVA.

**Bell witness.**– With the measurement settings defined in Eq. (21), the Bell operator reads

$$\hat{B}(\theta) = \cos^2(\theta)\hat{\Lambda}_0^2 + \sin(\theta)\hat{\Lambda}_1 + \sin^2(\theta)(n - \hat{n}_2) + 2\hat{n}_2, \quad (\text{F1})$$

which is written in terms of the collective Gell-Mann matrices  $\Lambda_a = \sum_{i \in [n]} \hat{\lambda}_a(i)$  and of the population onto level  $|2\rangle$ ,  $\hat{n}_2 = \sum_{i \in [n]} |2\rangle\langle 2|(i)$ .

In terms of the shorthand notation introduced in Eq. (22), the expectation value of Eq. (F1) is

$$\frac{\langle \hat{B}(\theta) \rangle}{nz} = \cos^2(\theta)x + \sin(\theta)y + \sin^2(\theta) + \frac{2(1-z)}{z}. \quad (\text{F2})$$

For  $y^2/30 \leq x \leq (2-y)/2$ , the optimal angle to minimize Eq. (F2) fulfills

$$\sin(\theta) = y/[2(x-1)]. \quad (\text{F3})$$

From Eq. (F2), we derive the inequality

$$2 - \beta + (2x-3)z + \sqrt{(\beta+z-yz-2)(\beta+z+yz-2)} \geq 0, \quad (\text{F4})$$

where  $\beta \leq \langle \hat{B} \rangle/n$ . For  $\beta = 0$ , we obtain the Bell correlation witness Eq. (23) (multiplied by  $z$ ). Similarly, for  $\beta = -1/4$ , one would obtain the dimension witness

$$9 + 4z(2x-3) + \sqrt{9^2 - 8z(9+2z(y^2-1))} \geq 0. \quad (\text{F5})$$

However, since the maximal violation of the Bell operator considered here is achieved by qubits, the dimension witness Eq. (F5) is trivial. Indeed, at the point of maximal violation  $z = 1$ , which results in  $8x + \sqrt{5^2 - (4y)^2} \geq 3$ . For a perfectly squeezed state,  $x = 0$  and  $y = 1$ , then,  $\sqrt{5^2 - 4^2} = 3$  is saturated.

**Wineland criterion.**– Here we illustrate a derivation of entanglement witness Eq. (24) of the main text. We start with the inequality

$$\frac{\langle \hat{\Lambda}_1 \rangle^2}{(\Delta \hat{\Lambda}_0)^2} \leq \frac{\langle \hat{\Lambda}_1 \rangle^2}{\langle \hat{\Lambda}_0^2 \rangle} \leq 4(\Delta \hat{\Lambda}_2)^2, \quad (\text{F6})$$

where  $(\Delta \cdot)^2 = \langle \cdot^2 \rangle - \langle \cdot \rangle^2$  is the variance. Eq. (F6) follows directly from Robertson uncertainty relation with the type-2 algebra  $[\Lambda_1, \Lambda_2] = 2i\hat{\Lambda}_0$ . We proceed to bound  $(\Delta \hat{\Lambda}_2)^2$  over separable states. By convexity, it is sufficient to consider pure product states  $\hat{\rho}_n = \bigotimes_{i \in [n]} |\psi_i\rangle\langle\psi_i|$

$$\begin{aligned} (\Delta \hat{\Lambda}_2)^2 &= \sum_{i \neq j} \underbrace{\langle \hat{\lambda}_2(i) \hat{\lambda}_2(j) \rangle_n}_{= \langle \hat{\lambda}_2(i) \rangle \langle \hat{\lambda}_2(j) \rangle} + \sum_i \langle \hat{\lambda}_2^2(i) \rangle - \sum_{i,j} \langle \hat{\lambda}_2(i) \rangle \langle \hat{\lambda}_2(j) \rangle \\ &= n(\Delta \hat{\lambda}_2)^2 \leq n, \end{aligned} \quad (\text{F7})$$

where in the last step we used  $(\Delta \hat{\lambda}_2)^2 = 1 - \langle |2\rangle\langle 2| \rangle - \langle |0\rangle\langle 0| + |1\rangle\langle 1| \rangle^2 \leq 1$  to bound the local variance. From this derivation, we conclude that for separable states

$$\frac{\langle \hat{\Lambda}_1 \rangle^2}{\langle \hat{\Lambda}_0^2 \rangle} \leq 4n, \quad (\text{F8})$$

which using the notation introduced in Eq. (22) yields Eq. (24) of the main text.

We may as well introduce the pseudospin squeezing parameter

$$\xi^{-2} = \frac{\langle \hat{\Lambda}_1 \rangle^2}{4n\langle \hat{\Lambda}_0^2 \rangle}, \quad (\text{F9})$$

such that entanglement witness Eq. (F8) reads  $\xi^{-2} \leq 1$ .

**Spin nematic squeezing in BECs.**– For the dynamics we consider, since the initial state  $|0\rangle^{\otimes n}$  is totally symmetric and the Hamiltonian is PI, we have that the state remains confined to the symmetric subspace at any time. Hence, we can compute expectation values in such a restricted subspace, which can be done efficiently for moderate system sizes  $n$ . Following the main text, we consider the type-2 subspace spanned by  $\{\hat{S}_x, 2\hat{Q}_{yz}, (\hat{Q}_{zz} - \hat{Q}_{yy})\}$ . The mean (pseudospin) orientation during the dynamics is  $\langle (\hat{Q}_{zz} - \hat{Q}_{yy}) \rangle$ , which plays the role of  $\langle \hat{\Lambda}_1 \rangle$  of the previous discussion. Now, we want to find the minimal fluctuations or the second moment orthogonal to the mean spin direction (squeezed orientation), which will be interpreted as  $\langle \hat{\Lambda}_0^2 \rangle$ . To this end, we consider the covariance matrix:

$$C = \begin{pmatrix} \langle \hat{S}_x^2 \rangle & 2\text{Re}\{\langle \hat{S}_x \hat{Q}_{yz} \rangle\} \\ 2\text{Re}\{\langle \hat{S}_x \hat{Q}_{yz} \rangle\} & 4\langle \hat{Q}_{yz}^2 \rangle \end{pmatrix}, \quad (\text{F10})$$

where  $\text{Re}\{\langle \hat{S}_x \hat{Q}_{yz} \rangle\} = \langle \hat{S}_x \hat{Q}_{yz} + \text{h.c.} \rangle/2$ .

The minimal eigenvalue of  $C$ ,  $\lambda_{\min}(C)$ , corresponds to the minimal variance  $\langle \hat{O}^2 \rangle = \lambda_{\min}(C)$  of  $\hat{O} = v_x \hat{S}_x + v_{yz} \hat{Q}_{yz}$ , with  $\mathbf{v}_{\min} = (v_x, v_{yz})$  the corresponding eigenvector.

From such data, we compute the spin-nematic squeezing parameter [c.f. Eq. (F9)]

$$\xi^{-2} = \frac{r^2}{4n\lambda_{\min}(C)}, \quad (\text{F11})$$

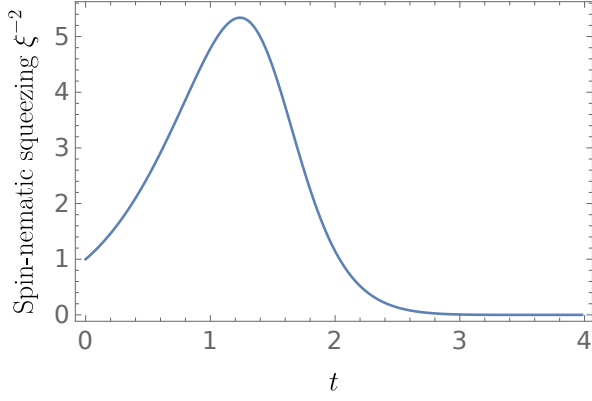


FIG. 6: Time evolution of the spin-nematic squeezing parameter Eq. (F11) for a system of  $n = 30$  particles initially prepared in polar state  $|0\rangle^{\otimes n}$  and then evolved according to Hamiltonian Eq. (25) of the main text. Here,  $c = -1$  and  $g = 0.2$ . Such a choice of parameters coincides with the one taken in Fig. 4 of the main text.

where  $r = \langle \hat{Q}_{zz} - \hat{Q}_{yy} \rangle$ .

We show in Fig. 6 the dynamics of the spin-nematic squeezing parameter  $\xi$ , for system initially prepared in the polar state  $|0\rangle^{\otimes n}$  and evolved with the spin-mixing Hamiltonian  $\hat{H} = c/(2n)\hat{\mathbf{S}}^2 + g\hat{Q}_{zz}$  [Eq. (25) of the main text].

From Fig. 6, we verify that at  $t = 0$ , the polar state saturates the spin-nematic squeezing parameter,  $\xi^{-2} = 1$ . Next, at short times, we observe generation of spin-nematic squeezing giving  $\xi^{-2} \geq 1$ . Finally, at longer times, over-squeezing results in a state with vanishing mean spin length, for which our witnesses are ineffective. The observation of spin-nematic squeezing in this model motivates us to verify the presence of Bell correlation through PIBI Eq. (4).

Recalling the optimal local measurements [c.f. Eq. (F3)]

$$\hat{m}_0 = \sqrt{1 - \frac{y^2}{4(x-1)^2}} \hat{\sigma} + \frac{y}{4(x-1)} (\hat{q}_{zz} - \hat{q}_{yy}) \quad (\text{F12})$$

$$\hat{m}_1 = \sqrt{1 - \frac{y^2}{4(x-1)^2}} \hat{\sigma} - \frac{y}{4(x-1)} (\hat{q}_{zz} - \hat{q}_{yy}) \quad (\text{F13})$$

which for our example result in the data

$$\begin{aligned} x &= \frac{\lambda_{\min}(C)}{n - \langle \hat{n}_\psi \rangle} \\ y &= \frac{r}{n - \langle \hat{n}_\psi \rangle} \\ z &= \frac{n - \langle \hat{n}_\psi \rangle}{n}, \end{aligned} \quad (\text{F14})$$

where  $\hat{n}_\psi = \sum_{i \in [n]} |\psi\rangle\langle\psi|^{(i)}$  and  $|\psi\rangle = (|0\rangle - |2\rangle)/\sqrt{2}$  is the projector orthogonal to the pseudospin subspace. Notice that  $|\psi\rangle\langle\psi| = (\hat{q}_{zz} + \hat{q}_{yy} - \hat{q}_{xx})/2$ . Hence, it can

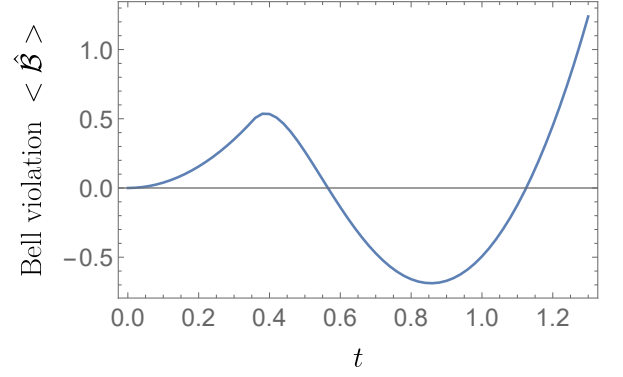


FIG. 7: Bell expectation value delivered by Eq. (4) against the time-evolved BEC state with in the same scenario as Figure (6). Values below zero (classical bound) entail Bell correlation. Note the change of the x-axis scale as compared to previous Figure 6.

also be expressed as  $\hat{n}_\psi = (\langle \hat{Q}_{zz} + \hat{Q}_{xx} - \hat{Q}_{yy} \rangle)/2$ . We plot in Fig. 7 the evolution of the Bell violation with optimized measurement settings. As expected, we observe that spin-nematic squeezing can be strong enough to allow for the detection Bell correlation.

#### Appendix G: Derivation of witness Eq. (28)

In this Appendix, we proceed to derive Eq. (28) of the main text.

**From probabilities to observables.**— We consider the following convention to label outcomes of the measurement operator  $\hat{m}_x$

$$\begin{aligned} \hat{m}_x &:= \hat{\pi}(0|x) - \hat{\pi}(1|x) \\ \hat{q}_{xx} &= \hat{\pi}(0|x) + \hat{\pi}(1|x) = \{\hat{m}_x, \hat{n}_x\}/2. \end{aligned} \quad (\text{G1})$$

Inverting the above relations, we obtain

$$\begin{aligned} \hat{\pi}(0|x) &= (\hat{q}_{xx} + \hat{m}_x)/2 \\ \hat{\pi}(1|x) &= (\hat{q}_{xx} - \hat{m}_x)/2. \end{aligned} \quad (\text{G2})$$

From here, one can rewrite Eq. (7) from moments of collective observables  $\hat{M}_x = \sum_{i \in [n]} \hat{m}_x^{(i)}$  (and collective moments of local observables,  $\hat{Q}_{xy} = \sum_{i \in [n]} \hat{q}_{xy}^{(i)}$ ,  $\hat{\mathfrak{Q}}_{xy} = (1/2) \sum_{i \in [n]} \hat{q}_{xx}^{(i)} \hat{q}_{yy}^{(i)} + \text{h.c.}$ ). For the one and two-body terms we have

$$\hat{\Pi}_{01|01} + \hat{\Pi}_{01|10} = \hat{\mathfrak{Q}}_{01} - \hat{Q}_{01} \quad (\text{G3})$$

$$2(\hat{\Pi}_{0|0} - \hat{\Pi}_{1|1})^2 + (\hat{\Pi}_{0|1} - \hat{\Pi}_{1|0})^2 = (\hat{M}_0 + \hat{M}_1)^2 + (\hat{Q}_{00} - \hat{Q}_{11})^2, \quad (\text{G4})$$

yielding

$$\hat{\mathcal{B}} = [(\hat{M}_0 + \hat{M}_1)^2 + (\hat{Q}_{00} - \hat{Q}_{11})^2]/2 + \hat{\mathfrak{Q}}_{01} - \hat{Q}_{01}. \quad (\text{G5})$$

**Probing spin-1 particles.**— Next, we exploit local spin-1 measurements along direction specified by  $\mathbf{r} \in \mathbb{R}^3$ , namely  $\hat{m} = \mathbf{r} \cdot \hat{\mathbf{s}}$ . As explained in the main text, we consider two measurement settings with angle  $2\theta$  between them

$$\begin{aligned}\hat{m}_0 &= \cos(\theta)\hat{s}_x + \sin(\theta)\hat{s}_y \\ \hat{m}_1 &= \cos(\theta)\hat{s}_x - \sin(\theta)\hat{s}_y\end{aligned}\tag{G6}$$

where  $\hat{s}_x$  and  $\hat{s}_y$  are spin-1 operators (or any SU(3) equivalent operators) along two orthogonal directions.

From these, we derive

$$\begin{aligned}\hat{q}_{00} &= c^2\hat{q}_{xx} + s^2\hat{q}_{yy} + 2cs\hat{q}_{xy} \\ \hat{q}_{11} &= c^2\hat{q}_{xx} + s^2\hat{q}_{yy} - 2cs\hat{q}_{xy} \\ \hat{q}_{01} &= c^2\hat{q}_{xx} - s^2\hat{q}_{yy} .\end{aligned}\tag{G7}$$

where we have used the shorthand notation  $c = \cos(\theta)$  and  $s = \sin(\theta)$ . These expressions are inserted into Eq. (G5), and the properties of  $\mathfrak{su}(3)$  matrices are used to linearize the anticommutators appearing in e.g.  $\hat{\mathcal{Q}}$ . As a result, the Bell operator reads

$$\begin{aligned}\hat{\mathcal{B}}(\theta) &= 2c^2\hat{S}_x^2 \\ &\quad - s^2c^2(3\hat{Q}_{zz} + \hat{Q}_{xx} - 8\hat{Q}_{xy}^2 - 2n\mathbb{I}) \\ &\quad + s^2(1 + s^2)\hat{Q}_{yy} .\end{aligned}\tag{G8}$$

The optimal angle  $\theta^*$  may be calibrated from the data  $\langle \hat{S}_x^2 \rangle := xn$ ,  $\langle 3\hat{Q}_{zz} + \hat{Q}_{xx} - 8\hat{Q}_{xy}^2 - 2n\mathbb{I} \rangle := yn$ ,  $\langle \hat{Q}_{yy} \rangle := zn$  and is set from  $s^2 = (2x + y - z)/[2(y + z)]$  in order to derive Eq. (28) from  $\langle \hat{\mathcal{B}}(\theta = \theta^*) \rangle \geq n\beta$ .